



HAL
open science

Responses of early life stages of European abalone (*Haliotis tuberculata*) to ocean acidification after parental conditioning: Insights from a transgenerational experiment

Stéphanie Auzoux-Bordenave, Apolline Ledoux, Sophie Martin, Carole Di Poi,
Marc Suquet, Aïcha Badou, Fanny Gaillard, Arianna Servili, Nelly Le Goïc,
Sylvain Huchette, et al.

► **To cite this version:**

Stéphanie Auzoux-Bordenave, Apolline Ledoux, Sophie Martin, Carole Di Poi, Marc Suquet, et al.. Responses of early life stages of European abalone (*Haliotis tuberculata*) to ocean acidification after parental conditioning: Insights from a transgenerational experiment. *Marine Environmental Research*, 2022, 181, pp.105753. 10.1016/j.marenvres.2022.105753 . hal-03797346

HAL Id: hal-03797346

<https://hal.science/hal-03797346>

Submitted on 24 Oct 2023

HAL is a multi-disciplinary open access archive for the deposit and dissemination of scientific research documents, whether they are published or not. The documents may come from teaching and research institutions in France or abroad, or from public or private research centers.

L'archive ouverte pluridisciplinaire **HAL**, est destinée au dépôt et à la diffusion de documents scientifiques de niveau recherche, publiés ou non, émanant des établissements d'enseignement et de recherche français ou étrangers, des laboratoires publics ou privés.

Responses of early life stages of European abalone (*Haliotis tuberculata*) to ocean acidification after parental conditioning: Insights from a transgenerational experiment

Auzoux-Bordenave Stéphanie ^{1,2,*}, Ledoux Apolline ³, Martin Sophie ^{2,4}, Di Poi Carole ³, Suquet Marc ³, Badou Aïcha ⁵, Gaillard Fanny ⁴, Servili Arianna ³, Le Goïc Nelly ³, Huchette Sylvain ⁶, Roussel Sabine ⁷

¹ UMR "Biologie des Organismes et Ecosystèmes Aquatiques" (BOREA), MNHN/CNRS/SU/IRD, Muséum national d'Histoire naturelle, Station marine de Concarneau, 29900, Concarneau, France

² Sorbonne Université, 4, place Jussieu, 75005, Paris, France

³ IFREMER, Université de Brest, CNRS, IRD, LEMAR, F-29280, Plouzané, France

⁴ UMR 7144 "Adaptation et Diversité en Milieu Marin" (AD2M), CNRS/SU, Station Biologique de Roscoff, 29680, Roscoff Cedex, France

⁵ Direction Générale Déléguée à la Recherche, l'Expertise, la Valorisation et l'Enseignement (DGD REVE), Muséum national d'Histoire naturelle, Station marine de Concarneau, 29900, Concarneau, France

⁶ Ecloserie France Haliotis, Kerazan, 29880, Plouguerneau, France

⁷ Université de Brest, CNRS, IRD, Ifremer, LEMAR, F-29280, Plouzané, France

* Corresponding author : Stéphanie Auzoux-Bordenave, email address :

stephanie.auzoux-bordenave@mnhn.fr

Abstract :

CO₂ absorption is leading to ocean acidification (OA), which is a matter of major concern for marine calcifying species. This study investigated the effects of simulated OA on the reproduction of European abalone *Haliotis tuberculata* and the survival of its offspring. Four-year-old abalone were exposed during reproductive season to two relevant OA scenarios, ambient pH (8.0) and low pH (7.7). After five months of exposure, abalone were induced to spawn. The gametes, larvae and juveniles were then exposed for five months to the same pH conditions as their parents. Several biological parameters involved in adult reproduction as well as in larval, post-larval and juvenile fitness were measured. No effects on gametes, fertilisation or larval oxidative stress response were detected. However, developmental abnormalities and significant decreases in shell length and calcification were observed at veliger stages. The expression profile of a GABA A receptor-like gene appeared to be regulated by pH, depending on larval stage. Larval and post-larval survival was not affected by low pH. However, a lower survival and a reduction of growth were recorded in juveniles at pH 7.7. Our results confirm that OA negatively impacts larval and juvenile fitness and suggest the absence of carry-over effects on abalone offspring. This may compromise the survival of abalone populations in the near future.

Highlights

► Abalone has experienced severe population decline worldwide due to overfishing, disease and climate change. ► OA effects were evaluated on reproduction and early life stages of *H. tuberculata* through a transgenerational experiment. ► No carry-over effects were observed on abalone offspring following parental exposure to OA. ► Larval and juvenile fitness were affected by a pH decrease of 0.3 unit. ► Species dispersion and survival may be compromised in the near future, with potential negative consequences for European abalone populations.

Keywords: European abalone, *Haliotis tuberculata*, ocean acidification, carry-over effects, developmental abnormality, shell growth, calcification, gene expression

1 **1. Introduction**

2 The absorption of anthropogenic carbon dioxide emissions by seawater is responsible for a
3 decrease in the pH of the global ocean, a process known as ocean acidification (Doney et al.,
4 2009; Gattuso et al., 2015; IPCC, 2014). Current projections suggest that, by the year 2100,
5 seawater pH will have decreased by 0.1 to 0.3 units, threatening marine calcifiers such as corals,
6 molluscs and echinoderms (Hendricks et al., 2010; Hofmann et al., 2010; Kroeker et al., 2013;
7 Widdicombe and Spicer, 2008; Wittmann and Pörtner, 2013). Molluscs are among the
8 invertebrates considered the most vulnerable to OA, with pronounced sensitivity at larval and
9 juvenile stages (Beniash et al., 2010; Gazeau et al., 2013; Melzner et al., 2009; Orr et al., 2005;
10 Przeslawski et al., 2015; Ross et al., 2011). In marine shelled molluscs, OA has been shown to
11 reduce larval survival, lengthen development time, alter morphology and/or impair shell
12 formation and calcification (Byrne et al., 2011; Byrne and Fitzner, 2019; Duquette et al., 2017;
13 Ellis et al., 2009; Fitzner et al., 2014; Gazeau et al., 2010; Kurihara 2008; Noisette et al., 2014).
14 Since many mollusc species are sources of commercially important foods, the negative impacts
15 of OA may also result in significant economic losses (Ekstrom et al., 2015; Gazeau et al., 2007).

16 Abalone are ecologically and economically important shelled gastropods, which are grazers
17 in the marine ecosystem and a delicacy for human consumers (Cook, 2016; Huchette and Clavier
18 2004). Many abalone species worldwide have experienced severe population decline due to
19 overfishing, disease and environmental perturbations such as global warming (Cook, 2016;
20 Nicolas et al., 2002; Travers et al., 2009). Understanding the effects of climate change on abalone
21 physiology is an important issue for the management of abalone populations in natural and
22 aquaculture environments (Aalto et al., 2020; Morash and Alter, 2015).

23 The European abalone *Haliotis tuberculata* (Linnaeus, 1758) is a commercially important
24 species in Europe, for which rearing over the whole life cycle is controlled in aquaculture
25 (Courtois de Viçose et al., 2007). The impacts of OA on several stages of *H. tuberculata* have
26 been well examined by experimental studies (Auzoux-Bordenave et al., 2020; Avignon et al.,

27 2020; Wessel et al. 2018). As with most marine molluscs, abalone have a pelago-benthic life
28 cycle with a larval planktonic stage followed by a critical metamorphosis into benthic juveniles,
29 making them highly sensitive to environmental changes (Byrne et al., 2011). Several studies have
30 also focused on early life stages of abalone, especially larvae, demonstrating adverse effects of
31 elevated CO₂, such as reduced survival, developmental delay, body and shell abnormalities and
32 reduced mineralization (Byrne et al., 2011; Crim et al., 2011; Guo et al., 2015; Kimura et al.,
33 2011; Onitsuka et al., 2018; Wessel et al., 2018; Zippay and Hofmann 2010). More recently,
34 Kavousi et al. (2021) investigated the combined effects of OA and ocean warming on *H.*
35 *tuberculata* larvae in a full factorial experiment. Despite no interaction between elevated
36 temperature and low pH being observed, the results provided additional evidence for the
37 sensitivity of abalone larvae to OA (Kavousi et al., 2021). Only one study has yet reared abalone
38 embryos in acidified conditions from the fertilisation stage (Byrne et al., 2011); this demonstrated
39 that resulting larvae were more severely affected by OA than those exposed at a later stage. In
40 all the above-mentioned papers, experiments were carried out on a single life-history stage using
41 short-term or acute exposure to pH decrease, that provided information on the vulnerabilities of
42 embryos and larvae (Parker et al., 2015; Ross et al., 2016). More recently, a multigenerational
43 experiment conducted on the red abalone *Haliotis rufescens* (Swezey et al., 2020) demonstrated
44 that larval mortality under OA was strongly correlated with differences in lipid provisioning and
45 metabolism. The differences were linked to population-specific variation in the maternal
46 provisioning of lipids with a positive correlation between lipid concentrations and survival under
47 lower pH. This relationship also persisted in experiments on second-generation animals (Swezey
48 et al., 2020), confirming the importance of parental exposure when studying the effects of OA.

49 To better understand the effects of OA on abalone reproduction and the survival of its
50 offspring, we carried out a 10-month transgenerational experiment exposing adult abalone to two
51 climatically relevant OA scenarios. Four-year-old abalone *H. tuberculata* were exposed during
52 reproductive season to ambient seawater pH (8.0) or to a lower pH value (7.7) corresponding to
53 the decrease of -0.3 pH units expected for the end of the century (RCP 8.5 climate change

54 scenario, Gattuso *et al.*, 2015; IPCC, 2014). The offspring resulting from the reproduction of
55 these adults were then kept in the same conditions and studied until the age of 5.5 months. Several
56 biological parameters involved in adult reproduction (gamete evaluation and fertilisation rate) as
57 well as larval, post-larval and juvenile fitness (survival, growth, calcification) were measured
58 throughout the experimental period. To our knowledge, this is the first study that examines the
59 acclimation potential of European abalone to simulated OA, considering carry-over effects being
60 transmitted from adults to their offspring.

61

62 **2. Material and Methods**

63 **2.1. Abalone collection and conditioning**

64 Adult *H. tuberculata* ($n = 260$, 48.5 ± 4.2 mm shell length) were selected at random from an
65 offshore sea-cage structure at the France Haliotis abalone farm ($48^{\circ}36'50\text{N}$, $4^{\circ}36'3\text{W}$;
66 Plouguerneau, Brittany, France) in January 2017, as previously described in Avignon *et al.*
67 (2020). These abalone were distributed without any selection among ten 45-L open-circuit aquaria
68 ($n = 26$ abalone per aquarium) supplied with a minimum of 15 L/h of 3 μm filtered seawater at
69 ambient temperature. They were conditioned for three weeks in the laboratory under ambient
70 pCO_2/pH conditions and fed *ad libitum* with the macroalgae *Palmaria palmata*.

71

72 **2.2. Experimental set-up**

73 The experimental system used to test the two pH treatments (ambient pH 8.0 and reduced pH
74 7.7) on adult abalone was previously described in detail in Avignon *et al.* (2020). Briefly, each
75 experimental aquarium ($n = 10$) was supplied from a separate header tank where pCO_2 was
76 adjusted by bubbling CO_2 (Air liquid, France) through electro-valves controlled by a pH-stat
77 system (IKS Aquastar, Germany). Five replicate aquaria, were used per pH condition. The adult
78 experiment was conducted for five months between January and June 2017, during reproductive
79 conditioning.

80 The maturity of the broodstock was checked during routine hatchery operations before
81 induction of spawning. After four months of exposure, 10 abalone per pH treatment were
82 sacrificed for the assessment of gonad maturity (Avignon et al. 2020). Experimental animals
83 were maintained for one additional month before spawning induction. At maturity (i.e. after five
84 months of exposure to pH treatments), adult abalone were induced to spawn using a temperature
85 shock of +4°C and UV-irradiated seawater. For ambient pH, 18 males and 19 females were used;
86 for reduced pH, 18 males and 16 females were used ($n = 3-4$ abalone of each sex per aquarium).
87 Abalone were placed individually in 1 L buckets with continuous water renewal at ambient pH
88 and allowed a maximum of 5:30 h from the start of the spawning induction in which to spawn.
89 During spawning induction, the pH was not adjusted,
90 due to the small volume of the buckets and to minimise the stress for abalone during spawning.
91 An experimenter continuously observed spawning behaviour to spot the onset of gamete
92 emission. Once the spawning started, the water renewal was halted to avoid gamete loss. When
93 they had finished spawning, the adults were removed from the buckets. The water containing the
94 gametes was gently stirred to ensure homogeneous distribution through the water column. Two
95 replicate samples of 0.4 ml were taken to estimate the number of gametes released by females
96 and males and to determine spermatozoon morphology. Oocytes were fixed in 70% ethanol and
97 spermatozoa in 2% glutaraldehyde. Furthermore, for analysis of spermatozoon movement, a
98 sample of 0.5 ml of male gametes was taken, placed in a microcentrifuge tube and transferred to
99 the Argenton laboratory within 45 min. Male gametes of abalone are known to be resistant to
100 transport, even without oxygenation (Pereira et al., 2007).

101 A full factorial fertilisation was carried out per aquarium. Gametes of each female were
102 transferred to 5-L buckets (two to four buckets of gametes per female depending on the number
103 of males from the same aquarium that spawned), which were topped up with seawater at pH 8.0
104 or pH 7.7 once the adults stopped spawning. Spermatozoa of each male were added to the buckets
105 containing the oocytes of the females from the same aquarium. To avoid spermatic competition,

106 this was done at an optimal ratio of approximately 100 000 spermatozoa / oocyte (Huchette et
107 al., 2004). Because oocytes are fragile, a maximum of 30 min was allowed between spawning
108 and fertilisation. Two minutes after fertilisation, three aliquots of 0.5 ml were taken per family
109 after gentle homogenisation of the bucket and placed in 12-well plates to study the percentage of
110 fertilisation per female. Ethanol (final concentration 70%) was added to the well after two hours
111 to block egg development until later analysis. Two hours after fertilisation, the 5-L egg buckets
112 of females from the same aquarium were pooled and placed in food-safe polystyrene boxes,
113 containing seawater of appropriate pH, until the eggs reached the hatching stage at about 18 hours
114 post fertilisation (hpf). To avoid flushing away any eggs, no water renewal was done during this
115 period. The pH was registered in the hatching boxes for the two pH treatments (n= 5 per pH
116 treatment). At 18 hpf, all swimming larvae were transferred through a pipe to 350-L larval tanks
117 supplied with filtered seawater (n = 5 tanks per pH treatment). Samples of larvae were taken from
118 the tanks at three key stages: (1) the trochophore stage (20 hpf), which is characterised by the
119 formation of the larval shell, to evaluate the initial number of swimming larvae; (2) the veliger
120 stage (48 hpf); and (3) the pre-metamorphic veliger stage (96 hpf), which is the last pelagic life
121 stage before larval settlement (Auzoux-Bordenave et al., 2010; Jardillier et al., 2008). At each
122 key stage, three 10-mL replicates were sampled per tank to measure the total number of
123 swimming larvae in each. In addition, 10–15 L of seawater were collected from the tank water
124 columns to study larval development and birefringence of larval shell. Collection of swimming
125 larvae in the water column allowed us to sample only live larvae from the tank. The larval
126 samples were then filtered through a 40- μ m sieve and aliquoted into 15-mL tubes. Larvae were
127 concentrated at the bottom of each tube by adding a few drops of 70% ethanol. The samples were
128 then fixed and stored in 70% ethanol until analysis.

129 Since abalone larvae are lecithotrophic, they were not fed during the experiment. At the end
130 of the planktonic phase (96 hpf), when the veliger larvae reached the pre-metamorphic stage, all
131 swimming larvae were collected from the 350 L tanks using a syphon and a 40- μ m sieve and

132 placed in buckets containing 5 L of seawater adjusted to the same pH as in their respective
133 treatments. The larval density at 96 hpf was calculated from eight 1-mL replicate samples per
134 bucket. After density evaluation, a total of 10 000 larvae was collected using a pipette and gently
135 poured into ten 45-L aquaria. These larvae were allowed to settle on 10 plastic plates covered
136 with the green alga *Ulvela lens*, which is a major inductive cue for the settlement of abalone
137 larvae (Courtois de Viçose et al. 2012; Daume et al., 2004). Post-larvae were sampled at 5 and 9
138 days after larval fixation on the plates and juveniles were collected at the mid-term (2.5 mo) and
139 end of the experiment (5.5 mo). By using this overall procedure, the juveniles sampled in one
140 aquarium corresponded to the offspring of the abalone of the same treatment conditioned in the
141 same aquarium.

142

143 **2.3. pH and carbonate parameters**

144 The desired low pH value was obtained by adjusting the pH to be 0.3 units lower than the
145 ambient pH value, which was characterised by natural pH fluctuations reported for coastal
146 seawater of northern Brittany (pH_T range of 7.9–8.2; Qui-Minet et al., 2018). The pH-stat system
147 values were adjusted from daily electromotive force measurements in the header tanks using a
148 pH meter (Metrohm 826 pH mobile, Metrohm AG, Herisau, Switzerland) with a glass electrode
149 (Metrohm, Primatrode, Switzerland). The electromotive force values were converted to pH units
150 on the total scale (pH_T) after calibration with Tris-HCl and 2-aminopyridine-HCl (AMP) buffers
151 (Dickson et al., 2007). Temperature and salinity were measured daily using a portable
152 conductivity meter (ProfiLine Cond 3110, WTW, Oberbayern, Germany).

153 Total alkalinity (AT) was measured monthly on 50-mL samples taken from each experimental
154 aquarium (n = 5 per pH treatment). Seawater samples were filtered through 0.7-µm Whatman
155 GF/F membranes, immediately poisoned with mercury chloride, and stored in a dark place at
156 room temperature for later analysis. Values of AT were then determined from approximately 50
157 g of weighed samples using a potentiometric titration at 25°C with 0.1 M HCl and an automatic

158 titrator (Titrimo 847 plus, Metrohm). The balance point was determined by the Gran method
159 (Gran, 1952), according to Haraldsson et al. (1997). The accuracy of this method was ± 2
160 $\mu\text{mol}\cdot\text{kg}^{-1}$ and was verified using Certified Reference Material 182, provided by A. Dickson
161 (Scripps Institute of Oceanography, University of South California, San Diego, United States).

162 The seawater carbonate chemistry analysis included dissolved carbonate (CO_3^{2-}), bicarbonate
163 (HCO_3^-), dissolved inorganic carbon (DIC), pCO_2 , aragonite saturation state ($\Omega_{\text{aragonite}}$) and
164 calcite saturation state (Ω_{calcite}). These values were determined by entering the values of pH_T , AT,
165 temperature and salinity into CO₂SYS software (Pierrot et al., 2006) using constants from
166 Mehrbach et al. (1973) as refitted by Dickson and Millero (1987).

167 The effects of reduced pH were examined at different sampling times corresponding to the
168 different life stages of abalone: gametes, eggs, larvae, post-larvae and juveniles. Several
169 biological parameters were measured at each life stage and compared between the pH treatments.

170

171 ***2.4. Number of gametes released and spermatozoon shape***

172 Oocytes were counted under a photonic microscope (Zoom 2000, Leica, Germany). For the
173 spermatozoon samples, SYBR Green fluorescent dye (4 μl , Molecular Probes, 10^{-3} dilution of
174 the commercial stock solution) was added before flow cytometry (Guava EasyCyte Plus
175 equipped with a 488-nm laser). Data were analysed using the Guava ExpressPro program. The
176 total number of spermatozoa was estimated as was their volume (Forward Scatter, FSC) and
177 complexity (Side Scatter, SSC). Duplicates were averaged per male ($n = 12$ males for pH 7.7; n
178 $= 15$ males for pH 8.0) and per female ($n = 14$ females for each pH level). Fecundity was
179 calculated as the number of oocytes and spermatozoa released per gram of abalone (wet weight)
180 that spawned (Bilbao et al., 2010).

181

182

183 **2.5. Spermatozoon motility**

184 Aliquots of 5 μL of spermatozoon suspension were diluted in 500 μL of activating solution
185 (1- μm fresh seawater, 0.3% pluronic acid, 15 mM Tris, pH 8.0., Boulais et al., 2018). Then, 12
186 μL of this diluted suspension were transferred to a Fast-Read 102 cell (Biosigma, Italy), and
187 spermatozoon movement was triggered under a microscope (Olympus BX51, X200
188 magnification) connected to a camera (Qicam Fsr 1394) as described in Boulais et al. (2015).
189 Two aliquots per male were analysed, with an average of 200 spermatozoa tracked (minimum of
190 56 spermatozoa observed per male).

191 The percentage of motile spermatozoa and their velocity (VAP: velocity of the average path)
192 were quantified using a CASA plug-in developed for ImageJ software adapted to Pacific oyster
193 spermatozoa (Boulais et al., 2015) and averaged per male. Calibration settings were defined as
194 follows: minimum spermatozoon size (pixels) = 1; minimum track length (frames) = 15;
195 maximum spermatozoon velocity between frames (pixels) = 8; minimum straight-line velocity
196 for motile spermatozoa ($\mu\text{m sec}^{-1}$) = 5; minimum VAP for motile spermatozoa ($\mu\text{m sec}^{-1}$) = 10;
197 minimum curvilinear velocity for motile spermatozoa ($\mu\text{m sec}^{-1}$) = 13; low VAP speed ($\mu\text{m sec}^{-1}$)
198 = 2; maximum percentage of path with zero VAP = 1; low VAP speed 2 ($\mu\text{m sec}^{-1}$) = 12; low
199 curvilinear velocity speed ($\mu\text{m sec}^{-1}$) = 15; and frame rate (frames sec^{-1}) = 25.

200

201 **2.6. Fertilisation percentage**

202 The number of eggs at 1-cell (non-fertilised eggs), 2-cell and 4-cell stages were counted with
203 a photonic microscope (Zoom 2000, Leica, Germany). The percentage of fertilisation
204 corresponds to the total number of cells at the 2- or 4-cell stages divided by the total number of
205 eggs counted. The fertilisation percentage was calculated for each female by averaging the value
206 obtained with the different males from the same aquarium ($n = 12$ for pH 7.7; $n = 15$ for pH 8.0).

207

208

209 **2.7. Larval survival**

210 The developmental timing was verified under a binocular microscope at 20, 48 and 96 hpf
211 before sampling the larvae. At each sampling time, the total number of swimming larvae was
212 estimated by counting the number of larvae under a binocular microscope. Larval survival at 48
213 hpf and 96 hpf was calculated with the following formula:

$$214 \quad \text{Larval survival} = (\text{total number of swimming larvae at } t+1) / 100 \times (\text{total number of} \\ 215 \text{ swimming larvae at } t)$$

216

217 **2.8. Slide preparation for larval morphometry and birefringence**

218 Larval samples were ethanol-fixed and whole-mounted on microscope slides for morphometry
219 and birefringence analysis. Microscope slides were prepared with ethanol-fixed larvae from the
220 different pH conditions, following the method described in Wessel et al. (2018). Larvae were
221 whole-mounted in about 500 μL of glycerol, keeping the amount of ethanol transferred to a
222 minimum. The slides were kept at room temperature for 5 to 10 min allowing the ethanol to
223 evaporate and the larvae to settle. Six spots of vacuum gel were deposited at the corners and
224 middle edges of a square coverslip to prevent the larvae from being crushed. After the coverslip
225 was placed over the larval samples, the slides were gently sealed with clear nail varnish. Each
226 slide contained approximately 100 larvae per treatment per larval stage.

227 Approximately 40 larvae per tank ($n = 200$ larvae per pH condition), regardless of their
228 orientation, shape and development were photographed with an Olympus binocular microscope
229 (Olympus, Hamburg, Germany) under phase contrast and polarized light. The same microscope
230 was equipped with polarizing filters for the birefringence analysis. Microscopic observations
231 were fully blinded to prevent bias arising from any a priori knowledge of larval treatment. All
232 images were taken with a digital camera (DS-R11, Nikon, Japan) at 20X magnification and 40-
233 ms exposure. Images were acquired with NIS-element and analysed using ImageJ software (v
234 1.52a).

235 **2.9. Morphometric analysis**

236 Tissue morphogenesis, shell formation and shell size were analysed on larvae lying laterally
 237 on their sides (n = 200 larvae per pH condition). A qualitative categorisation was used to assess
 238 larval morphology and growth according to the method previously developed for *H. tuberculata*
 239 larval assessment (Wessel et al., 2018). The phenotype of each larva was scored according to the
 240 following degrees of soft tissue morphogenesis and shell formation (see **Fig. 2** for more details):

241 - *Normal tissue development/ normal shell = normal phenotype*

242 - *Abnormal or partially developed tissues/ partial or no shell = altered phenotype*

243 The maximum larval length at 20 hpf and total shell length of fully shelled larvae at 48 and
 244 96 hpf were measured using ImageJ software and used as indicators of larval size, according to
 245 the method described in Kavousi et al. (2021) (**Fig. 1**). The mean larval length was calculated
 246 based on 40 larvae per tank (n = 200 per pH treatment).

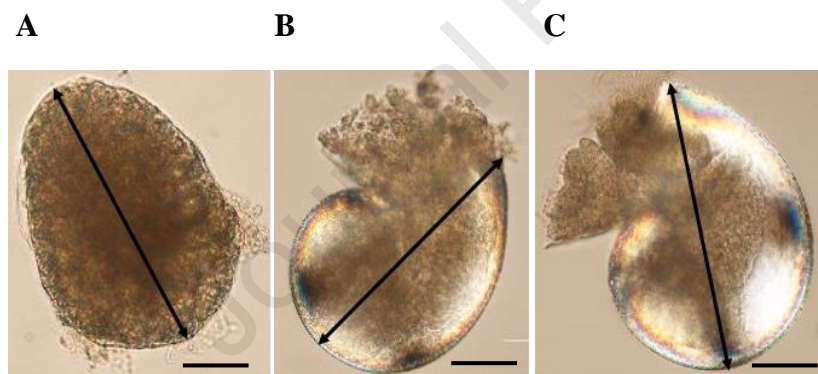


Fig. 1. Measurements of larval length at 20 hpf (A), and shell length at 48 hpf (B) and 96 hpf (C). Scale bar: 50 μ m

247 **2.10. Birefringence analysis**

248 Birefringence intensity has been previously used as a proxy for the assessment of CaCO₃
 249 mineralisation within the larval abalone shell (Kavousi et al., 2021; Wessel et al., 2018).
 250 Birefringence was measured on cross-polarized images taken of 48 and 96 hpf larval stages (n =
 251 200 per pH treatment). The younger 20 hpf larvae were not considered because the shell at this
 252 stage lacks sufficient crystallized CaCO₃ to calculate birefringence (Wessel et al., 2018). The
 253 mean greyscale level (0–255 pixels) was determined for each area of the larval shell showing

254 birefringence (i.e. 2 to 3 areas per larval shell). The values recorded for each area were averaged
255 into a global mean greyscale value, providing the birefringence intensity (in %) for each larval
256 shell.

257 **2.11. Oxidative stress**

258 Since OA and warming can cause significant alterations in cellular antioxidant responses
259 (Grilo et al., 2018; Zhang et al., 2021), three parameters related to oxidative stress, i.e. lipid
260 peroxidation, superoxide dismutase (SOD) and catalase, were measured in abalone larvae.

261 About 4000 larvae per tank (n = 5 tanks per treatment) were sampled at 96 hpf. The samples,
262 composed of larvae and seawater (200–300 μ L per tube), were flash frozen in liquid nitrogen and
263 then stored until analyses. These larval samples were then sonicated in two volumes of lysis
264 buffer (50 mM NaCl, 10 mM Tris, 1 mM EDTA, 1 mM EGTA, 1% Triton X-100, 0.5% Igepal,
265 1 tablet of complete EDTA-free protease inhibitor cocktail in 25 ml of buffer, phosphatase
266 inhibitor cocktail III) and centrifugated (45 min, 10 000 rpm, 4°C). The same lysates were used
267 for quantification of total proteins and parameters related to oxidative stress, i.e. lipid
268 peroxidation, superoxide dismutase (SOD) and catalase.

269 All enzyme assays were performed in triplicate in 96-well microplates (Nunc™, Thermo
270 Scientific) and read using a microplate reader (Bio-Tek® Synergy™ HT). Total proteins, MDA
271 and SOD were quantified using Gen5 software to compare the results with the calibration curves
272 provided with the respective assay kits. Total protein contents were quantified in each lysate (i.e.
273 1/10 dilution) according to Lowry et al. (1951) using the DC protein assay (Bio-Rad, Hercules,
274 CA, USA). Results are expressed in mg/mL.

275 Lipid peroxidation was approximated by MDA contents, quantified in the lysates (i.e. pure
276 samples) using the *OxisResearch*™ commercial kit (BIOXYTECH® MDA-586, TebuBio, Le
277 Perray-en-Yvelines, France) following the manufacturer's instructions. Results are expressed in
278 nmol per mg protein. Superoxide dismutase contents were quantified in the lysates (i.e. 1/10
279 dilution) using a CAS No. RN 905-89-1 commercial kit (S7446, Sigma Aldrich, Saint-Louis, MI,

280 USA) following the manufacturer's instructions. Results are expressed in units per mg protein
281 (U/mg), where 1 U of SOD is the amount of enzyme necessary to inhibit the formation of
282 xanthine/XO complex by 50%. Catalase activity was quantified in lysates at room temperature
283 following the method of Curd et al. (2019). Briefly, 10 μ L of pure samples were added to 195 μ L
284 of hydrogen peroxide solution (10 mM) to initiate the reaction. Absorbance was immediately
285 recorded every 15 s for 4 min using a Synergy HT microplate reader (BioTek, Winooski VT,
286 USA). CAT activity is expressed in mU/mg proteins, where 1 U is the amount of enzyme
287 necessary to catalyse 1 μ mole of H_2O_2 per minute (using $\epsilon_{H_2O_2}$, 39.4 $mM^{-1} cm^{-1}$).

288

289 **2.12. Gene expression analysis**

290 The expression profiles of selected genes were analysed in the abalone larvae at 48 and 96 hpf
291 (pooled per treatment from 5 tanks and corresponding to about 50 000 larvae/sample). The genes
292 were chosen with respect to their putative functions in shell biomineralization (lustrin A; carbonic
293 anhydrase 1, CA1; carbonic anhydrase 2, CA2) and neurosensory transmission (GABA A
294 receptor-like; serotonin receptor, 5HTR; **Table 1**). 18S-rRNA (18S) and elongation factor 1
295 (EF1) were chosen as reference genes. Specific primers for each gene were designed as detailed
296 in **Table 1**. To search for potential candidate hits for the GABA A receptor in *Haliotis*
297 *tuberculata*, tblastx (Basic Local Alignment Search Tool, NCBI) research was carried out using
298 the GABA A receptor sequence of *Haliotis asinina* (EF222254.1) as a query sequence against
299 the unfiltered transcriptome of *H. tuberculata* published by Harney et al. (2016). Then, blastx
300 (Basic Local Alignment Search Tool, NCBI) research against the non-redundant protein
301 sequences database was performed with all 38 candidate sequences previously obtained. The
302 sequence TR57267_c2_g1 (GenBank accession number GEAU01240864.1) was chosen as the
303 GABA A receptor-like sequence of *H. tuberculata* based on sequence similarities to the GABA
304 A receptor sequence of *Aplysia californica* (XP005111291.2). The *H. tuberculata* serotonin
305 receptor sequence (GEAU01264085.1) was identified by using serotonin receptor sequences
306 available in *Haliotis* against the unfiltered transcriptome of *H. tuberculata* (Harney et al., 2016).

307 The PCR products obtained with the primers targeting the serotonin receptor and the GABA
308 A receptor-like were sequenced to verify potential errors in the predicted sequences and primers.
309 The same primers were subsequently used in RT-qPCR to target the specific genes of the *H.*
310 *tuberculata* serotonin receptor and GABA A receptor-like sequence. Total RNA was extracted
311 from pools of larvae using Extract-all reagent (Eurobio, Courtaboeuf, Essonne, France) followed
312 by chloroform phase separation and isopropanol precipitation, including a step of DNase
313 treatment (RTS DNase Kit, MoBio). The concentration and quality of RNA were evaluated using
314 an ND-1000 NanoDrop® spectrophotometer (Thermo Scientific Inc., Waltham, MA, USA) and
315 an Agilent Bioanalyzer 2100 (Agilent Technologies Inc., Santa Clara, CA, USA). cDNA
316 synthesis was performed by reverse transcription (RT) using an iScript™ cDNA Synthesis kit
317 (Bio-Rad Laboratories Inc., Hercules, CA, USA) strictly following recommendations from the
318 supplier. Negative RT controls were performed for all samples (RT reaction without retro-
319 transcriptase enzyme). Transcript expression was quantified using the CFX96 Touch Real-Time
320 PCR Detection system (Bio-Rad Laboratories Inc.) according to the protocol previously
321 described by Mazurais et al. (2020). The relative quantity of messenger was normalized with the
322 Δ Ct method using the same CFX Manager software (Bio-Rad Laboratories Inc.).

323

324 ***2.13. Evaluation of post-larvae and juveniles***

325 Survival at settlement was evaluated at 9 days and 2 months after settlement. Biometric
326 measurements of juvenile abalone were performed at 2.5 and 5.5 mo of exposure to the different
327 pH conditions. At 2.5 months, 2-3 juveniles were sampled per aquarium. To avoid experimenter
328 bias during collection, a first individual was randomly observed on the plate. The next closest
329 one was then sampled, and images were taken with a digital camera (DS-Ri1, Nikon) and size
330 was analysed using ImageJ software (1.52a) with 0.01 mm precision. At the end of the
331 experiment (i.e. at 5.5 months of age), all the surviving abalone were photographed and sized
332 using digital imaging. The shells were weighed to the nearest 0.01 mg using an analytical balance.

Table 1. Specific primers used for gene expression analysis of *Haliotis tuberculata* larvae: GenBank accession number, primer sequences and references.

Gene	Accession number	Sequence 5'-3'	References
<i>Lustrin A</i>	HM852427.2	F-ATCTGTCCGGCAGTTCCTAC R-CTGGGGCACTGTAAGTTGGT	Gaume <i>et al.</i> (2014)
<i>Carbonic anhydrase 1</i>	HQ845770.1	F-ATGGCAGCTGATAAAGCAAC R-AGGGAAATGAGTGTGCATGT	Avignon <i>et al.</i> (2020)
<i>Carbonic anhydrase 2</i>	HQ845771.1	F-CGCCGACTTTATCTGAGAGC R-GTCTCCCACGAAGTGGTTGT	Le Roy <i>et al.</i> (2012)
<i>18S</i>	AF120511.1	F-GGTTCCAGGGGAAGTATGGT R-AGGTGAGTTTTCCCGTGTTG	Gaume <i>et al.</i> (2014)
<i>EF1</i>	FN566842.1	F-ATTGGCCACGTAGATTCTGG R-GCTCAGCCTTCAGTTTGTCC	Gaume <i>et al.</i> (2014)
<i>GABA A receptor-like sequence</i>	GEAU01240864.1	F-GCACACCGAGTGTGAGAAGA R-CAACACTGAATGTGGCGAAC	Designed for this study
<i>Serotonin receptor</i>	GEAU01264085.1	F-GCTACCACGACGACCATATC R- CCTTTCACGCTTTAGTTCCA	Designed for this study

333

334 **2.14. Statistical analysis**

335 All statistical analyses were performed with R software (R Core Team, 2015). Differences in
336 fertilisation rate, larval survival, total length, shell birefringence, and juvenile length, width and
337 weight were tested using the linear mixed model (LMM) with the lmerTest package (Kuznetsova
338 *et al.*, 2017) based on the method described by Winter (2013). This model used pH as a fixed
339 factor and aquarium as a random factor nested within pH. The normality of residuals and
340 homogeneity of variances were verified using Shapiro–Wilk tests and Levene tests based on
341 medians, respectively. When assumptions of homogeneity of variances and normal distribution
342 of residuals were not confirmed, the data were log or inverse transformed before analysis. If these
343 assumptions were not validated, generalized linear mixed models were applied using the GLMM
344 package with gamma inverse family for continuous data (Knudson *et al.*, 2021) with Wald Chi-
345 squared tests. If the GLMM model failed to converge, a non-parametric Welch test was

346 performed using the mean value per aquarium. To compare MDA, enzyme activities, gene
347 expression and juvenile survival between the two pH treatments, Student t-tests were used. A
348 Wilcoxon test was applied to 9-day post-larvae survival because non-normality of data was
349 observed. The morphological parameters of the larvae were evaluated using a Chi-squared (χ^2)
350 homogeneity test. Differences were considered significant at $p < 0.05$. Data are presented as least
351 square means of squares \pm standard error of means unless otherwise indicated.

352 **3. Results**

353 **3.1. Seawater parameters**

354 Mean seawater carbonate chemistry parameters for the different periods (i.e. the reproductive
355 period and the larval and juvenile period) of abalone exposure to the pH treatments are given in
356 **Table 2.**

357 During the reproductive conditioning (January to June 2017), seawater temperature followed
358 natural variations and ranged from $12.6^\circ\text{C} \pm 0.7^\circ\text{C}$ at the start of the experimental period to
359 $19.2^\circ\text{C} \pm 0.2^\circ\text{C}$ at the end. Salinity was 34.6 ± 0.6 in all experimental aquaria and remained stable
360 over the experiment. Total alkalinity (AT) measured in the experimental tanks was $2355 \pm 9 \mu\text{Eq.}$
361 kg^{-1} and remained stable throughout the experiment and among all aquaria. The seawater pH_T
362 was maintained close to the nominal value throughout the experiment, with 8.01 ± 0.05 (pCO_2
363 $439 \pm 57 \mu\text{atm}$) in the ambient pH aquaria and 7.71 ± 0.06 (pCO_2 $951 \pm 138 \mu\text{atm}$) in the low pH
364 aquaria. In pH 8.0 and pH 7.7 conditions, $\Omega_{\text{aragonite}}$ was 2.30 ± 0.31 and 1.25 ± 0.19 and Ω_{calcite}
365 was 3.59 ± 0.46 and 1.95 ± 0.28 , respectively (**Table 2**).

366 During the larval and juvenile period (July to December 2017), the seawater temperature
367 ranged from $19.2^\circ\text{C} \pm 0.2^\circ\text{C}$ at the start to $10.5^\circ\text{C} \pm 0.05^\circ\text{C}$ at the end of the experiment. Salinity
368 over the larval/juvenile period was 35.2 ± 0.2 in all experimental aquaria and remained stable
369 throughout the experiment. Total alkalinity (AT) was $2323 \pm 19 \mu\text{Eq. kg}^{-1}$ and remained stable
370 throughout the experiment and among all aquaria. The mean pH_T was 8.10 ± 0.06 (pCO_2 : $351 \pm$

371 54 μatm) in ambient pH aquaria and 7.71 ± 0.03 (pCO_2 : $951 \pm 138 \mu\text{atm}$) in low pH aquaria. In
 372 pH 8.0 and pH 7.7, $\Omega_{\text{aragonite}}$ was 2.78 ± 0.41 and 1.26 ± 0.13 and Ω_{calcite} was 4.32 ± 0.63 and 1.97
 373 ± 0.19 conditions, respectively (**Table 2**).

Table 2. Seawater pH_T temperature and parameters of the carbonate system in each pH treatment (i.e., pH 8.0. and pH 7.7, $n = 25$ per pH treatment). Seawater pH on the total scale (pH_T), temperature, salinity and total alkalinity (AT) were used to calculate CO_2 partial pressure (pCO_2 ; μatm), dissolved inorganic carbon (DIC; $\mu\text{mol}/\text{kg}$), HCO_3^- ($\mu\text{mol}/\text{kg}$), CO_3^{2-} ($\mu\text{mol}/\text{kg}$), aragonite saturation state ($\Omega_{\text{aragonite}}$) and calcite saturation state (Ω_{calcite}) by using the CO_2SYS program. Values are means \pm s.d.

Experimental period	Nominal pH	pH_T	Temperature ($^\circ\text{C}$)	AT ($\mu\text{mol}\cdot\text{kg}^{-1}$)	pCO_2 (μatm)	DIC ($\mu\text{mol}\cdot\text{kg}^{-1}$)	HCO_3^- ($\mu\text{mol}\cdot\text{kg}^{-1}$)	CO_3^{2-} ($\mu\text{mol}\cdot\text{kg}^{-1}$)	$\Omega_{\text{aragonite}}$	Ω_{calcite}
Reproductive period ¹ (5 months)	8.0	8.01 ± 0.05	14.4 ± 1.4	2355 ± 9	439 ± 57	2150 ± 28	1984 ± 48	151 ± 20	2.30 ± 0.31	3.59 ± 0.46
	7.7	7.71 ± 0.06	14.4 ± 1.5	2355 ± 9	951 ± 138	2277 ± 25	2154 ± 30	82 ± 12	1.25 ± 0.19	1.95 ± 0.28
Larval and juvenile period ² (5.5 months)	8.0	8.10 ± 0.06	15.4 ± 2.2	2323 ± 19	351 ± 54	2069 ± 41	1875 ± 64	181 ± 26	2.78 ± 0.41	4.32 ± 0.63
	7.7	7.71 ± 0.03	15.3 ± 2.1	2323 ± 19	966 ± 69	2237 ± 15	2119 ± 20	83 ± 8	1.26 ± 0.13	1.97 ± 0.19

¹Data from Avignon *et al.* 2020; ² 5 time points per month ($n = 25$ per treatment)

374 3.2. Gametes and fertilisation

375 The number of gametes released (oocytes and spermatozoa) per gram of abalone was not
 376 different between individuals exposed to pH 8.0 and pH 7.7 (**Table 3**). No significant differences
 377 in spermatozoon characteristics (i.e. SSC, FSC, percentage of motile spermatozoa and velocity)
 378 were observed between abalone exposed to pH 8.0 and pH 7.7 ($p > 0.05$, **Table 3**). In addition,
 379 fertilisation success was not significantly different between low and ambient pH ($p > 0.05$, **Table**
 380 **3**).

381

382 3.3. Larval survival

383 Survival did not differ between larvae exposed to pH 8.0 and 7.7 at 48 hpf or 96 hpf (survival
 384 at 48 h for pH 8.0 vs pH 7.7: $9.3 \pm 1.69\%$ vs $12.7 \pm 2.32\%$, $t = 1.165$, $df = 8$, $p = 0.2778$; survival

385 at 96 h for pH 8.0 vs pH 7.7: $78.8 \pm 17.83\%$ vs $56.2 \pm 11.74\%$, $t = -1.057$, $df = 8$, $p = 0.321$,
 386 Student t-test, mean \pm s.e.).

387

Table 3. Number of gametes released, spermatozoon characteristics and percentage of fertilisation of abalone *H. tuberculata* after 5 months of low (7.7) or ambient (8.0) pH exposure. ^α Linear mixed model analysis with the Satterthwaite method otherwise stated. ^βGLMM analysis fit by maximum likelihood (Laplace approximation) with gamma inverse family and Wald Chi-squared test with no over-dispersion. Least square mean \pm s.e.m. presented.

	pH 8.0	pH 7.7	F	p-value
Number of gametes released				
Number of oocytes released/g ^α	4187 \pm 623	3708 \pm 625	F _{1,10.7} = 0.295	0.598
Millions of spermatozoa released/g ^α	885 \pm 164.7	857 \pm 163.4	F _{1,9.0} = 0.015	0.906
Spermatozoa shape and motility				
SSC (complexity) ^α	326 \pm 10.3	315 \pm 10.0	F _{1,9.0} = 0.628	0.449
FSC (volume) ^α	180 \pm 2.9	179 \pm 2.9	F _{1,8.9} = 0.045	0.836
Percentage of motile spermatozoa (%) ^α	64.0 \pm 0.03	56.9 \pm 0.03	F _{1,26} = 2.241	0.146
Velocity (μ m/s) ^α	75.6 \pm 1.44	74.0 \pm 1.44	F _{1,26} = 0.626	0.436
Gamete fertilisation success				
Fertilisation percentage (%) ^β	53.1 \pm 5.55	62.9 \pm 6.26	$\chi^2 = 0.814$, $df = 1$	0.361

388 3.4. Larval morphology

389 At 20 hpf, larvae exposed to pH 7.7 showed less alteration of tissue organogenesis than those
 390 exposed to pH 8.0 (25% for pH 7.7 vs 43% for pH 8.0, $\chi^2 = 15.2$, $p < 0.001$, Pearson Chi-squared
 391 test). On the contrary, 20 hpf-larvae showed a significant increase in shell abnormalities at pH
 392 7.7 compared with larvae reared in ambient conditions (69% for pH 7.7 vs 59% for pH 8.0, $\chi^2 =$
 393 4.31, $p = 0.038$, Pearson Chi-squared test, **Fig. 2A**).

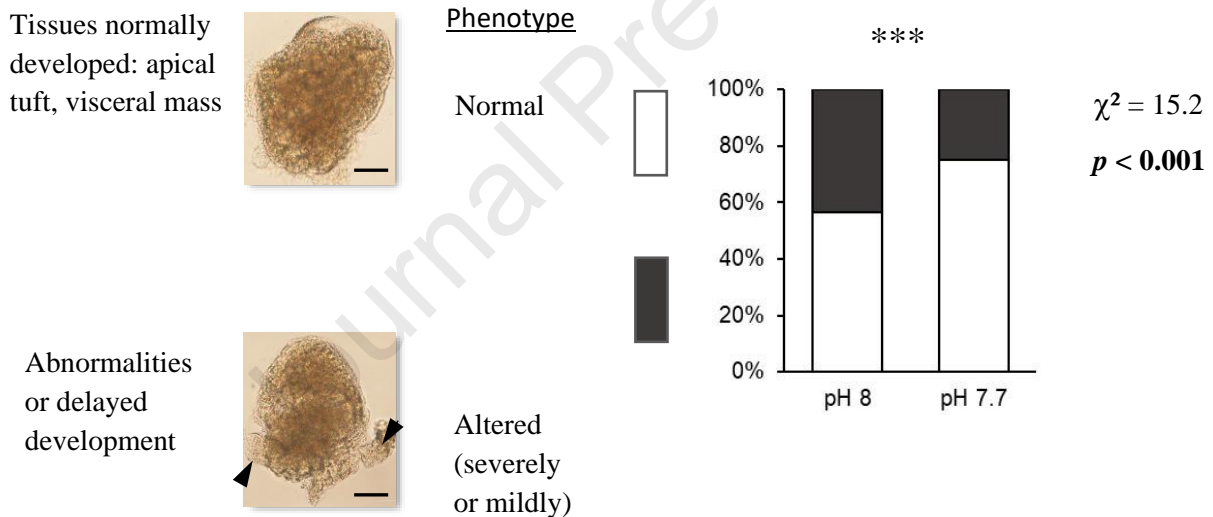
394 At 48 hpf, larvae exposed to pH 7.7 showed more tissue abnormalities than larvae exposed to
 395 pH 8.0 (75% for pH 7.7 vs 64% for pH 8.0, $\chi^2 = 6.27$, $p = 0.012$, Pearson Chi-squared test). In
 396 addition, larvae exposed to pH 7.7 showed a significant increase in shell abnormalities compared

397 with those reared in ambient pH conditions (97% for pH 7.7 vs 83% for pH 8.0, $\chi^2 = 20.7$, $p <$
 398 0.001, Pearson's Chi-squared test, **Fig. 2B**).

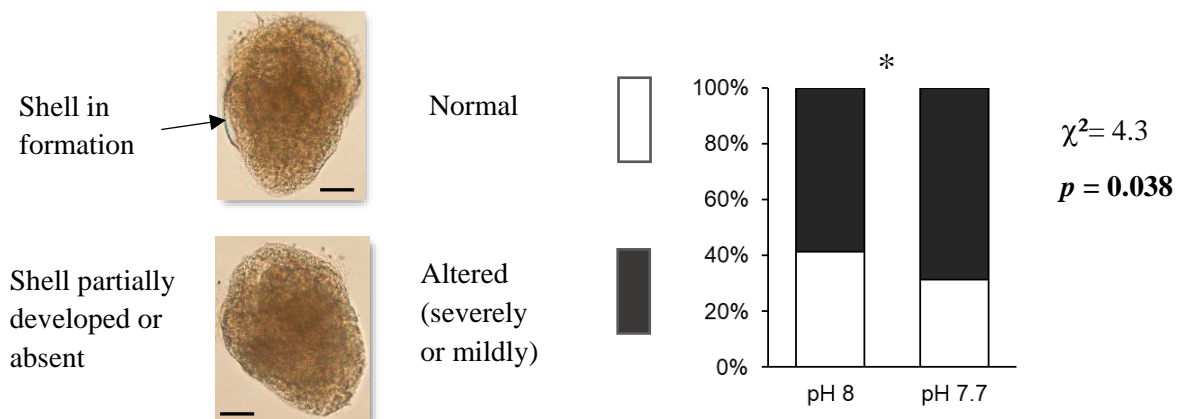
399 At 96 hpf, larvae exposed to pH 7.7 had more tissue abnormalities than those exposed to pH
 400 8.0 (8.5% for pH 7.7 vs 3% for pH 8.0, $\chi^2 = 5.58$, $p = 0.018$, Pearson Chi-squared test). Shell
 401 formation was also affected by lower pH, with a significant increase in shell alterations at pH 7.7
 402 compared with larvae reared in ambient pH conditions (97% for pH 7.7 vs 85% for pH 8.0, $\chi^2 =$
 403 16.56, $p < 0.001$, Pearson Chi-squared test, **Fig. 2C**).

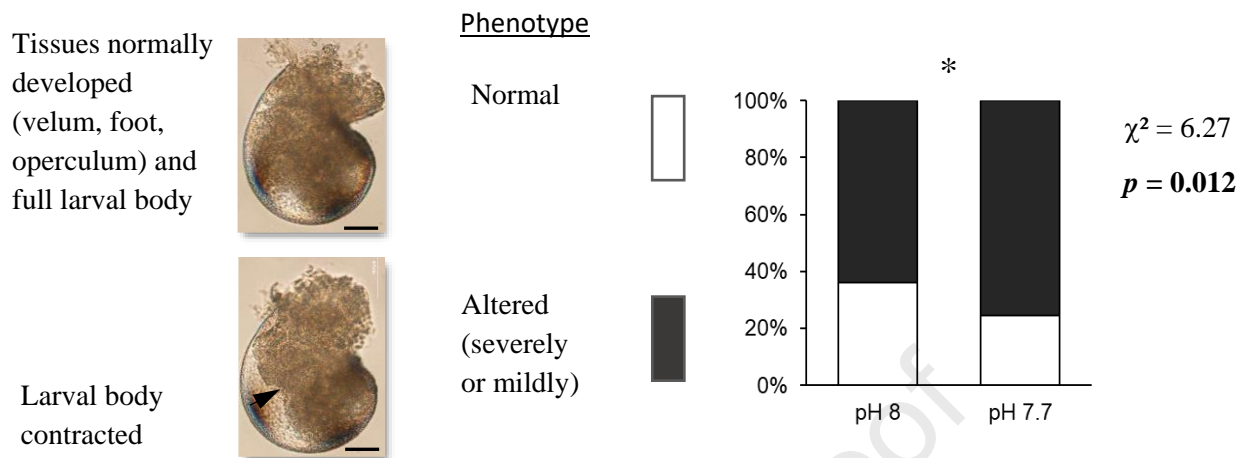
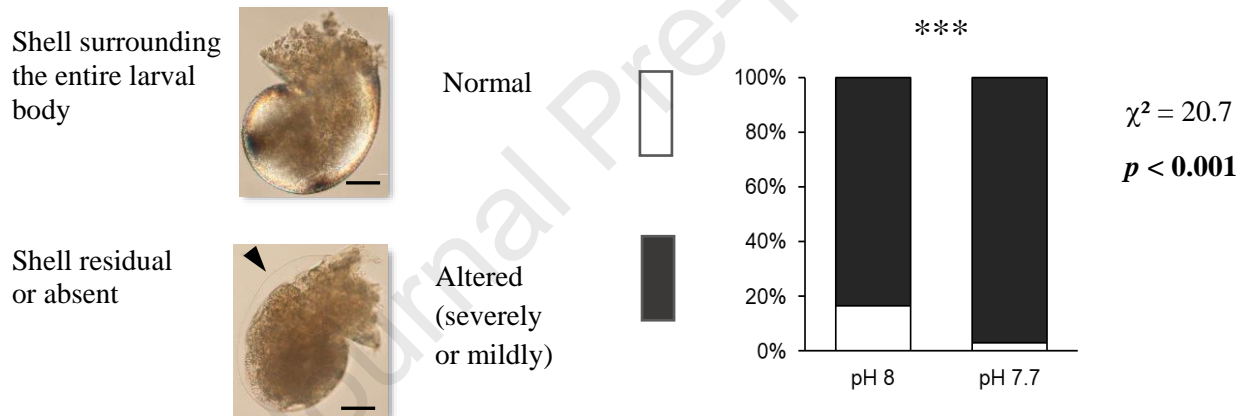
A. 20 hpf larvae

SOFT TISSUE MORPHOGENESIS



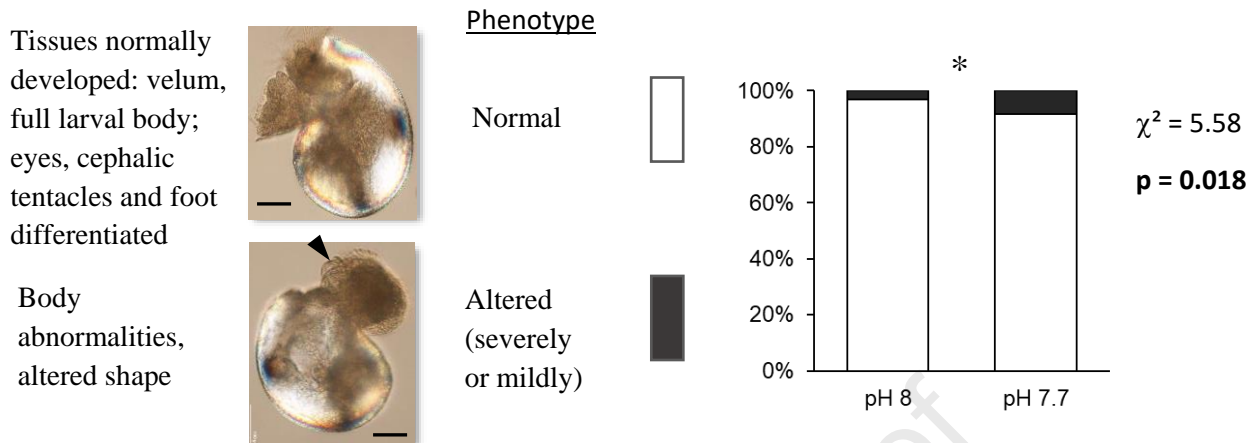
SHELL FORMATION



B. 48 hpf larvae**SOFT TISSUES****SHELL**

C. 96 hpf larvae

SOFT TISSUES



SHELL

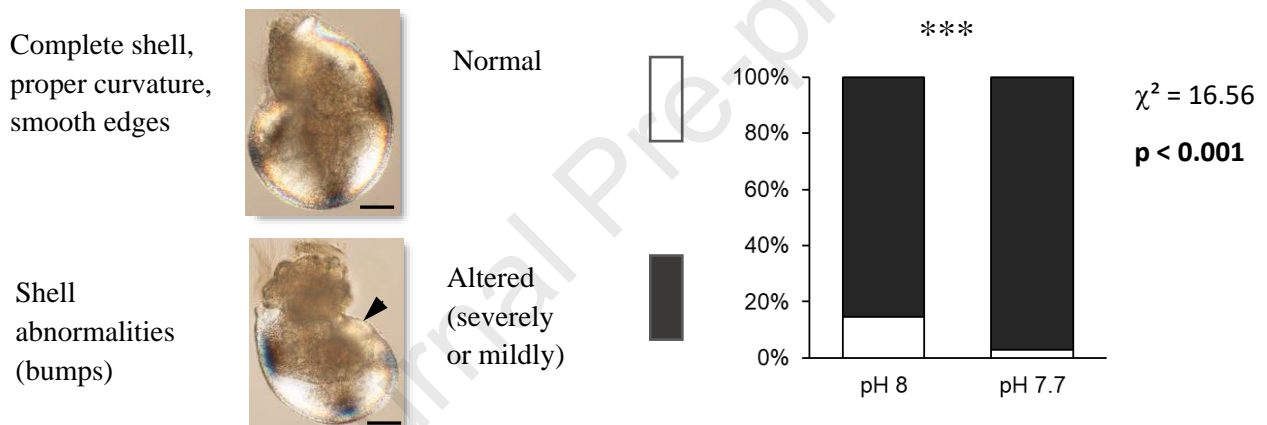


Fig. 2. Percentage of larvae (%) presenting either normal (white squares) or altered phenotypes (black squares) based on the degree of soft tissue morphogenesis and shell formation after exposure to two pH conditions (8.0 and 7.7). (A) 20 hpf, (B) 48 hpf and (C) 96 hpf (n = 200 larvae per pH treatment, Chi-squared test). Arrowheads in the pictures indicate body or shell abnormalities. Scale bar: 50 μ m.

404 **3.5. Larval length**

405 No differences were observed in larval length at 20 hpf or shell length at 48 hpf between larvae
 406 exposed to pH 8.0 and pH 7.7 (20 hpf: $\chi^2 = 0.197$, df = 1, $p = 0.657$; 48 hpf: $\chi^2 = 0.250$, df = 1,
 407 $p = 0.617$, GLMM analysis with gamma inverse family). However, larvae exposed to pH 7.7 had
 408 a smaller shell length at 96 hpf than larvae exposed to pH 8.0 ($\chi^2 = 10.13$, df = 1, $p = 0.001$,
 409 GLMM analysis with gamma inverse family) (**Fig. 3**).

410

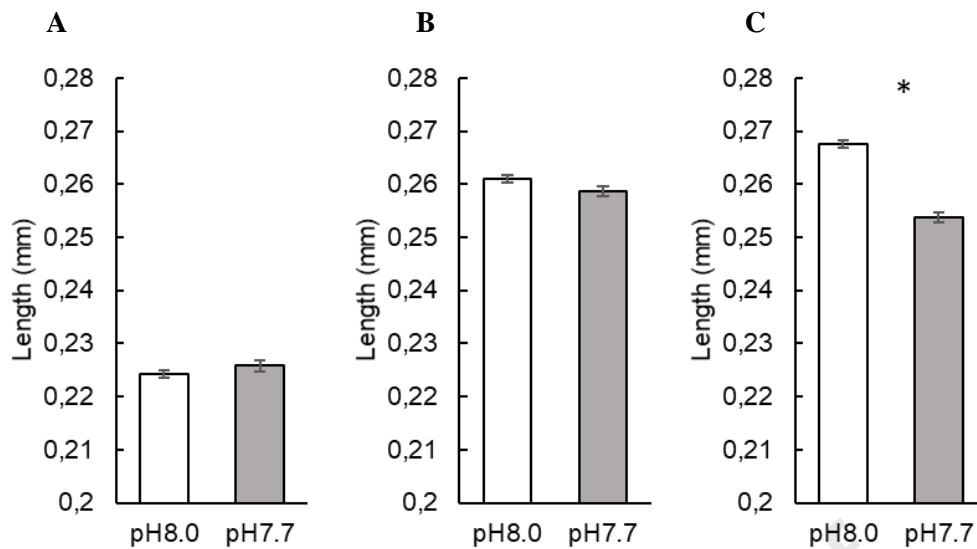


Fig. 3. Length of *H. tuberculata* larvae reared under ambient (pH 8.0) and low pH (7.7) at (A) 20 hpf, (B) 48 hpf and (C) 96 hpf (n = 200 larvae per pH treatment, n = 5 tanks per treatment). Larvae were exposed to the same pH as their parents. Ls mean \pm s.e.m. * $p < 0.05$ (GLMM analysis with gamma inverse family).

411 3.6. Birefringence analysis

412 The mean birefringence (corresponding to shell calcification level) of the larval shell at 48 h
 413 did not differ significantly between individuals from the two pH treatments ($F_{1,10} = 3.28$, $p =$
 414 0.099, LMM analysis, **Fig. 4A**). However, shell birefringence at 96 hpf was significantly lower
 415 in the pH 7.7 treatment than in control larvae in ambient conditions at pH 8.0 ($F_{1,10} = 7.46$, $p =$
 416 0.021, LMM analysis, **Fig. 4B**).

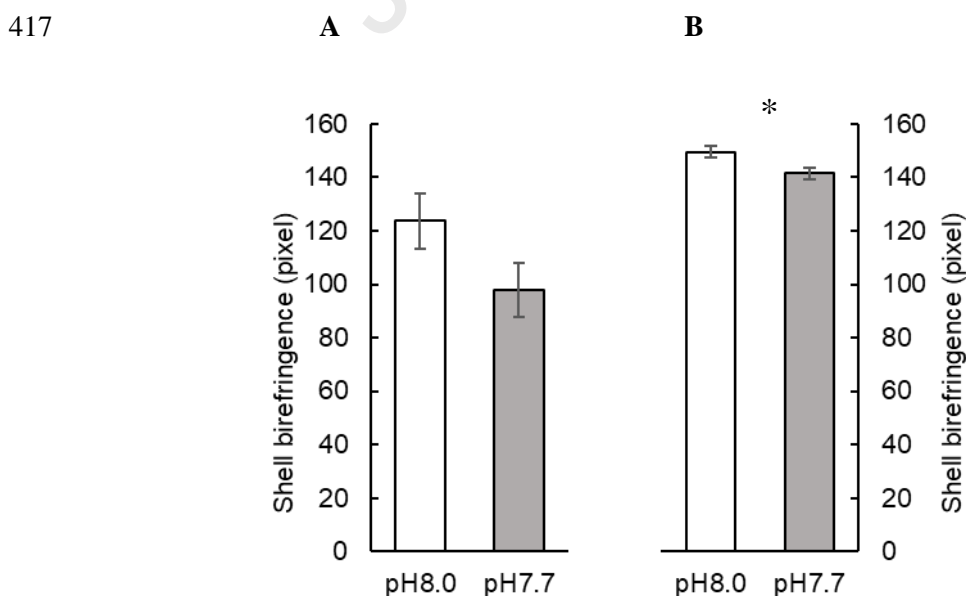


Fig. 4. Mean shell birefringence (number of greyscale pixels) of *H. tuberculata* larvae reared under ambient (pH 8.0) and low pH (7.7) at (A) 48 hpf and (B) 96 hpf. Larvae were exposed to the same pH as their parents. Ls mean \pm s.e.m. * $p < 0.05$ (LMM analysis).

418 **3.7. Oxidative stress**

419 No difference in catalase activity was observed between 96hpf-larvae exposed to pH 8.0 and
420 pH 7.7 (2.25 ± 0.428 vs 2.09 ± 0.408 mU/mg prot, respectively, $t = -2.26$, $df = 8$, $p = 0.800$,
421 Student t-test, mean \pm s.e.), MDA (1.14 ± 0.181 vs 1.28 ± 0.152 nmol/mg prot, respectively, $t =$
422 -0.549 , $df = 8$, $p = 0.598$, Student's t-test, mean \pm s.e.) or SOD activity (5.78 ± 1.370 vs $6.48 \pm$
423 0.139 U/mg prot, respectively, $t = 0.370$, $df = 5$, $p = 0.727$, Student t-test, mean \pm s.e.). Due to
424 the small number of larvae contained in the samples, SOD could not be analysed for two samples
425 from pH 7.7 and one sample from pH 8.0.

426

427 **3.8. Gene expression**

428 At 48 hpf, larvae exposed to pH 7.7 tended to have higher GABAAR-like gene expression
429 than larvae exposed to pH 8.0 ($t = -2.29$, $df = 8$, $p = 0.051$, Student t-test). No difference was
430 observed for 5HTR or CA2 gene expression between larvae exposed to the two pH treatments (t
431 $= -0.209$, $df = 8$, $p = 0.840$ and $t = -0.46111$, $df = 5$, $p = 0.6641$, respectively, Student t-test; **Fig.**
432 **5A**).

433 At 96 hpf, larvae exposed to pH 7.7 showed a downregulation of GABAAR-like gene expression
434 ($t = 2.43$, $df = 7$, $p = 0.046$, Student t-test) and tended to have lower 5HTR gene expression ($t =$
435 -2.16 , $df = 7$, $p = 0.068$, Student t-test) compared with larvae exposed to pH 8.0. No significant
436 difference was observed in CA2 gene expression levels ($t = -0.38$, $df = 7$, $p = 0.712$, Student t-
437 test, **Fig. 5B**). The expression levels quantified for CA1 and lustrin A genes were below the
438 detection limit for both larval stages.

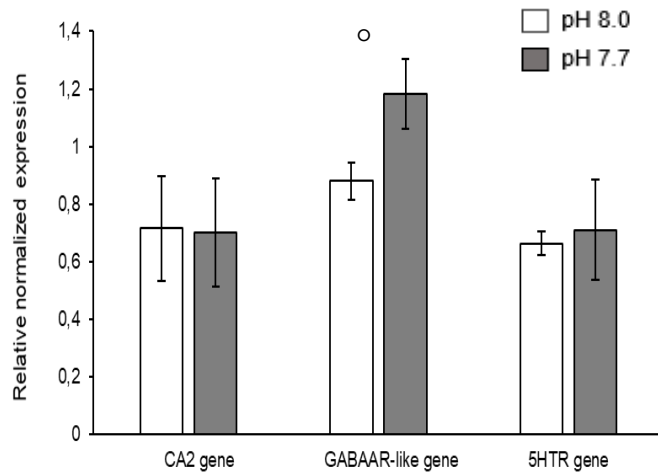
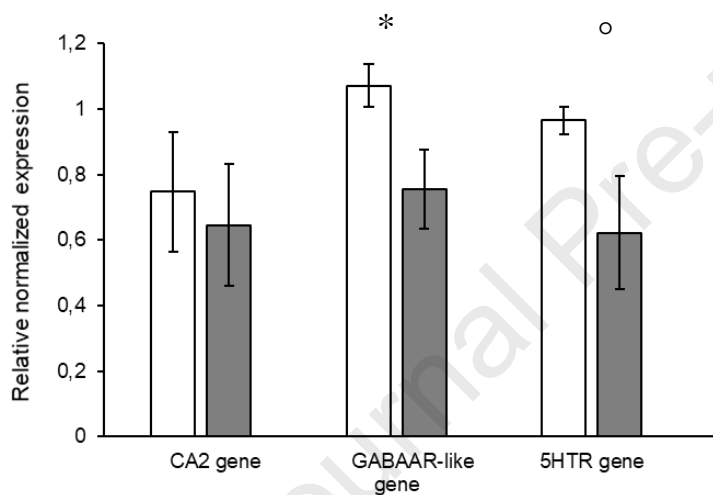
A**B**

Fig. 5. Expression patterns of CA2, GABAAR-like and 5HTR genes of abalone larvae exposed to ambient (pH 8.0) and low pH (7.7). A: 48 hpf and B: 96 hpf. Larvae were exposed to the same pH as their parents. Mean \pm s.e. * $p < 0.05$, ^o $p < 0.10$ (Student t-test).

3.9. Post-larval and juvenile evaluation

439 The main characteristics of abalone post-larvae at 9 days after settlement are shown in **Fig. 6**.
 440 After metamorphosis, the post-larval shell shows a well-defined transition between protoconch
 441 (pr) and newly deposited sculptured, juvenile shell (js).

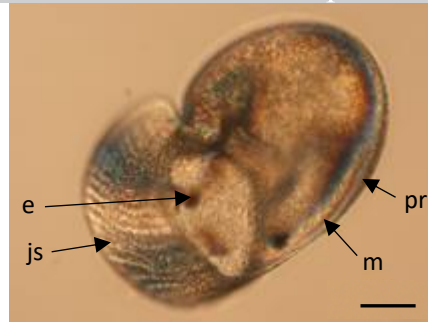


Fig. 6. Microscopic image of post-larval abalone *H. tuberculata* 9 days after settlement. The post-larval shell shows a well-defined transition between the protoconch (pr) and the newly deposited juvenile shell (js). Eyes (e) and mantle (m) are visible through the thin protoconch shell (pr). Scale-bar: 50 μ m.

442 No significant difference in abalone survival was observed between the two pH treatments 9
 443 days after settlement ($W = 17$, $p = 0.42$, Wilcoxon test, **Fig. 7A**). However, the survival of post-
 444 larvae two months after settlement was significantly lower for individuals grown at pH 7.7
 445 compared with those grown at pH 8.0. (13% and 46%, respectively, $t = -3.02$, $df = 8$, $p = 0.017$,
 446 Student t-test; **Fig. 7B**).

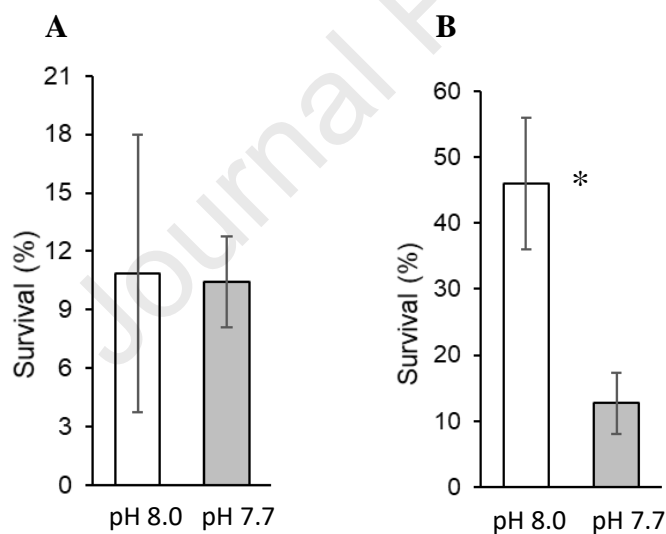


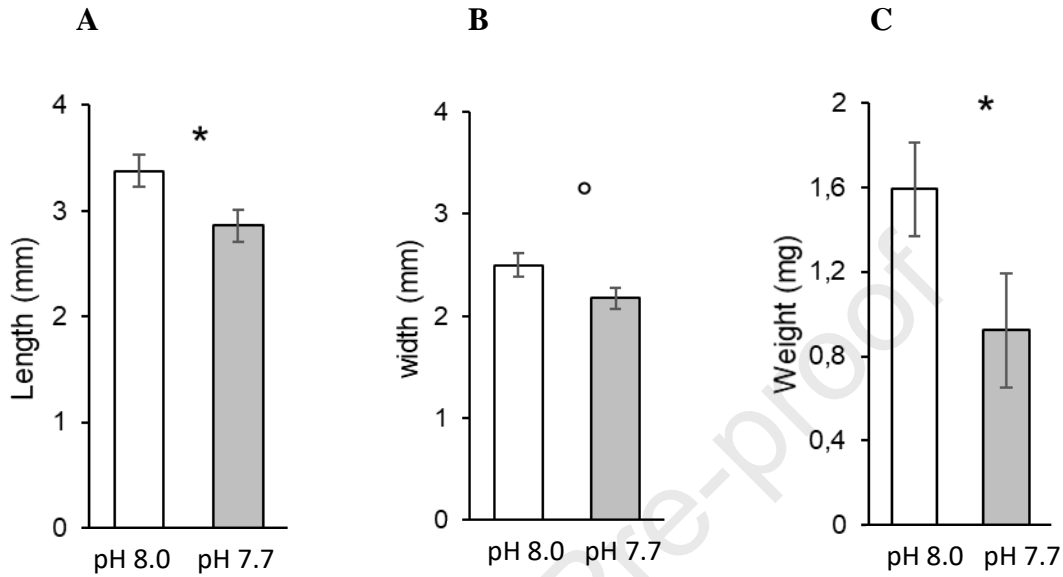
Fig. 7. Survival of abalone post-larvae 9 days (A) and 2 months after settlement (B) in the two pH treatments (pH 8.0 and 7.7). Post-larvae were exposed to the same pH as their parents. Mean \pm s.e. * $p < 0.05$ (Student t-test).

447 At 2.5 months, juveniles exposed to pH 7.7 had a lower length ($F_{1, 9.9} = 5.89$, $p = 0.036$, LMM
 448 analysis), tended to have a lower width ($F_{1, 9.6} = 4.34$, $p = 0.065$, LMM analysis) and were lighter
 449 in weight ($F_{1, 5.2} = 6.94$, $p = 0.045$, log transformation, LMM analysis) compared with juveniles
 450 kept at ambient pH (**Fig. 8 A–C**). At 5.5 months, shell length ($F_{1, 21} = 16.56$, $p < 0.001$, LMM
 451 analysis), width ($F_{1, 20} = 19.78$, $p < 0.001$, LMM analysis) and weight ($F_{1, 3.9} = 21.33$, $p < 0.001$,

452 LMM analysis) were also significantly lower in juvenile abalones exposed to pH 7.7 than in those
 453 exposed to ambient pH (Fig. 8 D–F).

454

2.5 months



5.5 months

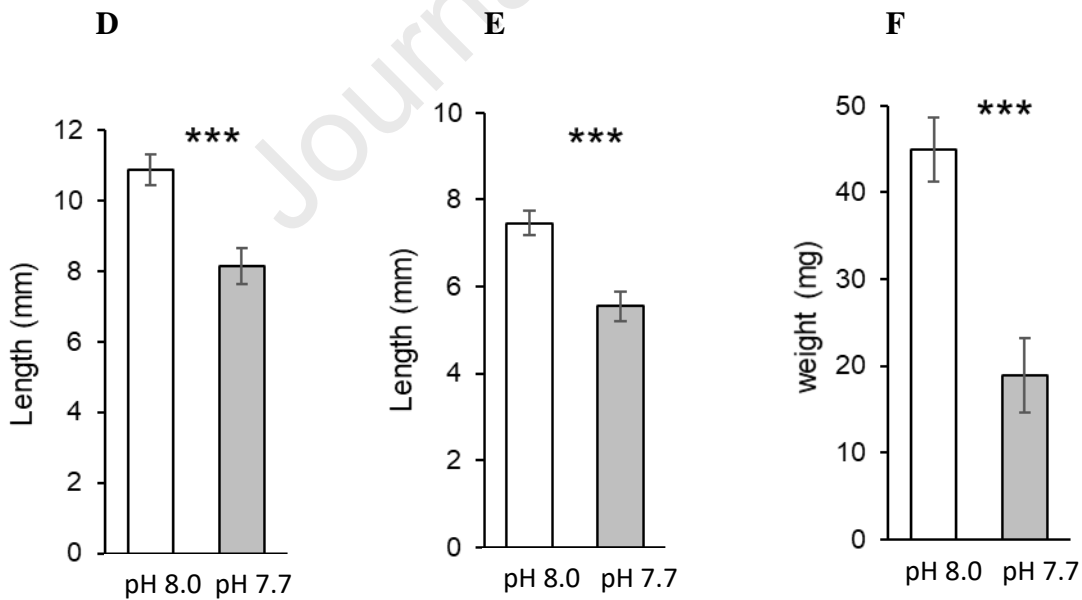


Fig. 8. Shell length (A, D), width (B, E) and weight (C, F) of 2.5-month-old and 5.5-month-old abalones *H. tuberculata* in the two pH treatments (pH 8.0 and 7.7). Juveniles were exposed to the same pH as their parents. Ls mean \pm s.e.m. * $p < 0.05$; ° $p < 0.10$

455 4. Discussion

456 This study investigated for the first time the effect of ocean acidification on the European
457 abalone *Haliotis tuberculata* by following transgenerational exposure to two relevant OA
458 scenarios (ambient pH and -0.3 pH unit decrease). Although the gametes and the fertilisation rate
459 appeared unaffected by the decreased pH, several biological parameters involved in larval and
460 juvenile fitness (survival at settlement, growth and calcification) were reduced at pH 7.7,
461 suggesting a high sensitivity of abalone offspring exposed to the same pH conditions as their
462 parents.

463 In adult *H. tuberculata*, no significant differences in gamete quantity or quality were found
464 between the two pH treatments after five months of reproductive conditioning. In the same way,
465 the fertilisation rate was not affected by this pH difference, suggesting that fertilisation success
466 and resulting embryos are tolerant of OA. Such tolerance to pH stress in the early life stages has
467 already been reported for many other species, including abalones (Byrne et al., 2010, 2011;
468 Przeslawski et al., 2015). In early embryos of sea urchins, it has been suggested that the resilience
469 to acidification stress might be due to protective proteins accumulated in the egg during
470 embryonic development (Hamdoun and Epel, 2007). In *H. tuberculata*, the magnitude of OA (-
471 0.3 pH units) is probably below the tolerance threshold of abalone embryo physiology.

472 Furthermore, our results reveal that the survival of abalone larvae was not affected by a 0.3
473 pH unit decrease, as previously shown in 30 hpf *H. tuberculata* (Wessel et al., 2018). A recent
474 multigenerational study on the red abalone *H. rufescens* demonstrated that larval mortality under
475 OA was strongly correlated with differences in the maternal provisioning of lipids with a positive
476 correlation between lipid concentration and survival under OA (Swezey et al., 2020). This
477 relationship was maintained in experiments on second-generation animals. Our results agree with
478 previous studies showing that early embryonic and larval stages are less vulnerable to pH stress
479 than later stages (Przeslawski et al., 2015; Swezey et al., 2020). Indeed, later veliger stages (48
480 and 96 hpf) of *H. tuberculata* exhibited a higher sensitivity to lower pH (7.7) with an increase of

481 developmental abnormalities, a decrease in length and reduced calcification, as previously shown
482 in single-stage experiments on *H. tuberculata* larvae (Kavousi et al., 2021; Wessel et al., 2018).
483 Such effects of OA have been already reported in marine mollusc larvae, as differences in
484 sensitivity to pH stress according to stage of development (Gazeau et al., 2013; Przeslawski et
485 al., 2015).

486 Our results did not, however, reveal any induction of oxidative stress response in 96 hpf
487 veliger larvae exposed to the lowest pH, which overall showed no change in lipid peroxidation
488 or similar antioxidant enzyme activities compared to control larvae. Yet, it has previously been
489 demonstrated that ocean acidification and warming can cause significant alterations in cellular
490 parameters related to antioxidant responses in marine gastropods (Grilo et al., 2018; Zhang et al.,
491 2021). Here, the lack of antioxidant response highlights the ability of abalone larvae to counteract
492 potential oxidative stress induced by OA, even though they showed developmental artefacts at
493 96 hpf. Nevertheless, few studies have considered oxidative stress parameters as key factors in
494 assessing the susceptibility of mollusc larvae to near-future OA. There are only, to our
495 knowledge, two studies of this kind, which were done on clams (Gurr et al., 2021; Munari et al.,
496 2016).

497 Although responses vary among marine organisms, the expression of genes involved in
498 calcification, ion regulation, metabolism and behaviour have been shown to be influenced by
499 decreased pH (Strader et al., 2020). To better understand the molecular processes involved in
500 larval responses to OA, the present study investigated the expression profiles of genes involved
501 in shell biomineralization (carbonic anhydrases CA1, CA2 and shell matrix lustrin A) on two
502 larval stages (48 and 96 hpf). Only CA2 expression levels could be quantified in larval extracts
503 and these did not show any regulation by pH treatment at the two larval stages studied. These
504 results are consistent with those previously reported in adult *H. tuberculata*, where CA
505 expression in the mantle did not vary across pH treatments (Avignon et al., 2020). In their study
506 on larval red abalone *Haliotis rufescens*, Zippay and Hofmann (2010) also found that decreased

507 pH did not affect the expression pattern of two shell formation genes in any abalone larval stages.
508 Although calcification gene expression showed no significant changes between pH treatments,
509 larval shells showed significant alterations or a delay in development in individuals reared at low
510 pH. These results support the hypothesis that the effects on shell formation may be mainly due
511 to a direct effect of low pH on shell dissolution, as previously shown in juvenile and adult stages
512 of *H. tuberculata* (Auzoux-Bordenave et al., 2020; Avignon et al., 2020).

513 As in vertebrates, GABA and serotonin signalling are major players in the nervous systems of
514 gastropod molluscs, where they are involved in the control of motor activity and cognitive
515 processes such as memory and learning (Aonuma et al. 2020; Miller, 2019;), but their specific
516 role during larval development has not been clarified in abalone. GABA A receptors have often
517 been proposed as responsible for the disruption of sensory transduction at the central level
518 observed in fish exposed to OA (Nilsson et al., 2012). This hypothesis has only recently been
519 extended to invertebrate species (Thomas et al., 2020). GABA is a ligand-gated ion channel
520 permeable to chloride and bicarbonate ions and acts as a major inhibitory neurotransmitter in the
521 central nervous system. In acidified seawater, because of the alteration of chloride and
522 bicarbonate concentrations across the neuronal cells, GABA would act as stimulatory
523 neurotransmitter (Nilsson et al., 2012). In the present study, the expression profile of two genes
524 involved in neurotransmission and behaviour (GABA A receptor-like and serotonin receptors)
525 were also analysed in abalone larvae exposed to OA conditions. Interestingly, the results showed
526 that GABA A receptor-like was upregulated in 48 hpf larvae under lower pH but was
527 downregulated in 96 hpf larvae in the same conditions. This could indicate that the genetic
528 response of abalone to OA changes with ontogenetic stage. In several gastropod species, GABA
529 signalling is involved in the induction of settlement and metamorphosis (Hatakeyama and Ito,
530 2000; Hernádi, 1994; Jing et al., 2003; Lerusalimsky and Balaban, 2001). In our experimental
531 conditions (temperature 15–16°C), the settlement of *H. tuberculata* larvae occurred around 96
532 hpf, which is consistent with the opposite regulation shown for GABA A receptor-like at 48 and

533 96 hpf. Interestingly, the expression pattern of the serotonin receptor gene in abalone larvae
534 broadly follows the one described for the GABA A receptor-like gene, at least at 96 hpf. This is
535 in line with the observation that certain invertebrates possess a serotonin-gated chloride channel
536 that may respond to an increase of pCO₂ in the same way as the GABA A receptor (Thomas et
537 al., 2020).

538 Our results also showed that pH decrease did not have any impact on post-larval settlement 9
539 days after fertilisation. These results are consistent with previous findings in *H. tuberculata*
540 (Kavousi et al., 2021) and *H. kamtschatkana* (Crim et al., 2011), but contrast with two other
541 studies, in the New Zealand abalone *H. iris* and the donkey's ear abalone, *H. asinina*, both of
542 which showing a lower settlement rate of larval abalone under low pH conditions (Espinel-
543 Velasco et al., 2021; Tahil and Dy, 2016). These contrasting effects among *Haliotis* species may
544 be due either to differences in larval sensitivity or to other indirect effects of decreased pH on the
545 settlement substrate, as previously shown in abalone larvae (O'Leary et al., 2017).

546 Juveniles maintained at pH 7.7 showed an increase of mortality at 2.5 months and significant
547 reductions in total length, width and weight at 5.5 months. These results are consistent with those
548 previously obtained on farmed abalone species including *H. tuberculata* (Auzoux-Bordenave et
549 al., 2020; Cunningham et al., 2016; Li et al., 2018). In juvenile *H. iris*, Cunningham et al. (2016)
550 reported significant effects on shell length and wet weight at lower pH_T (0.3 to 0.5 units below
551 ambient pH). Similarly, shell growth and shell weight were significantly decreased in juvenile
552 *H. discus hannai* (Li et al., 2018) after 3 months of exposure to lower seawater pH (0.2 units
553 below ambient pH). In six-month-old *H. tuberculata*, our previous studies revealed significant
554 reductions in juvenile shell length, weight and strength in a pH 7.6 treatment (0.5 units below
555 ambient pH) after three months of exposure (Auzoux-Bordenave et al., 2020). Furthermore, the
556 decrease in shell strength and changes in texture and porosity of the biomineral layers suggested
557 that low pH induced both general effects on growth mechanisms and corrosion of the carbonated
558 shell in *H. tuberculata*.

559 Transgenerational experiments, in which parents are exposed to low pH conditions during
560 reproductive conditioning, are currently performed to measure how this parental exposure may
561 influence the responses of the offspring (Parker et al., 2015). For most of the species studied to
562 date, especially bivalves, transgenerational exposure to OA resulted in positive carry-over effects
563 being transmitted from adults to their offspring, influencing the resilience of molluscs to OA
564 (Fitzer et al., 2014; Parker et al., 2015; Ross et al., 2016; Swezey et al., 2020). In the oyster *S.*
565 *glomerata*, the exposure of adults to reduced pH (0.3 unit below ambient pH) during reproductive
566 conditioning resulted in positive carry-over effects on larvae, including faster development and
567 increased growth, compared with larvae spawned from adults reared at ambient pH (Parker et al.,
568 2012). When the transgenerational exposure was repeated on the next generation (F2), an
569 increase in the resilience of the larval and juvenile offspring was observed (Parker et al., 2015).
570 These experiments demonstrate that marine molluscs may have the ability to acclimate or adapt
571 to future acidification of seawater through transgenerational pathways.

572 In the present study, the adverse effects of seawater acidification on larval and juvenile F1
573 abalone are in the range of those already observed in previous single-stage experiments (Auzoux-
574 Bordenave et al., 2020; Kavousi et al., 2021; Wessel et al., 2018). The absence of significant
575 carry-over effects on the offspring following parental exposure to OA suggests that larval
576 dispersion of *H. tuberculata* in the natural environment may be at greater risk under pH stress,
577 with potential negative consequences for abalone populations. However, considering the short
578 duration of the abalone larval stage (5 days) and the huge morphological and physiological
579 changes that occur concomitantly, it cannot be excluded that some transgenerational mechanisms
580 may mitigate the adverse effects of OA on abalone larvae by acting on other biological variables
581 or developmental processes that were not investigated in the present study.

582

583

584 In conclusion, this study demonstrated that OA may have detrimental consequences for
585 abalone populations in natural and aquaculture environments. Because abalone is a slow-growing
586 gastropod with a long transgenerational period, the possibility for this species to adapt to OA is
587 probably lower than that of fast-growing molluscs with rapid life cycles. Consequently, wild
588 abalone populations that are already weakened by anthropogenic pressure (e.g. pollution,
589 overfishing and diseases), will probably be the most at risk over the next decades. In abalone
590 aquaculture, various strategies could be developed to mitigate the effects of OA and help farmers
591 to overcome the challenges posed by climate change. For example, the introduction of macroalgal
592 culture into abalone farming (through IMTA system, Bolton et al., 2009) might be helpful to
593 increase pCO₂ in seawater intake and control the pH in nursery tanks, enabling an upstream
594 protection of the most vulnerable stages. In parallel, the identification of heritable traits involved
595 in resilience to OA, and the subsequent selection of tolerant broodstock may be exploited in the
596 future to ensure the sustainable development of abalone aquaculture.

597

598 **Acknowledgements**

599 This work was partially supported by the program *Acidification des Océans* (ICOBio project)
600 funded by the *Fondation pour la Recherche sur la Biodiversité* (FRB) and the *Ministère de la*
601 *Transition Ecologique et Solidaire* (MTES), the French LabexMER program (OASYS project)
602 and the ATM program IMADO of the MNHN funded by the *Ministère délégué à l'Enseignement*
603 *Supérieur et à la Recherche* (Paris, France). We are grateful to all the staff of the France Haliotis
604 farm (Plouguerneau) for hosting the experiment, to Manon Coheleach (University of Western
605 Brittany, Brest) and Thomas Bisch (AgroParisTech, Paris) for their help during abalone rearing
606 and measurements, and to Claudie Quéré (IFREMER, University of Western Brittany CNRS,
607 IRD, LEMAR) for biochemical analyses. Finally, we thank the Translation Bureau of the
608 University of Western Brittany for improving the English of this manuscript.

609

610 **Author contributions**

611 Stéphanie Auzoux-Bordenave, Sophie Martin, Sabine Roussel, Sylvain Huchette:

612 Conceptualization, Methodology, Validation;

613 Sabine Roussel, Sylvain Huchette: Investigation, Abalone breeding;

614 Stéphanie Auzoux-Bordenave, Apolline Ledoux, Sophie Martin, Aïcha Badou: Carbonate

615 chemistry analysis, Abalone sampling, Biological measurements;

616 Apolline Ledoux, Carole Di Poi : Oxidative stress measurements;

617 Carole Di Poi, Nelly Le Goïc, Marc Suquet : Gamete analysis;

618 Arianna Servili and Fanny Gaillard: mRNA extraction and gene expression

619 Stéphanie Auzoux-Bordenave, Sabine Roussel: Formal analysis, Visualization, Supervision,

620 Funding, Writing-Original Draft, Reviewing and Editing

621

622 **Declaration of competing interest.** The authors have no conflicts of interest to declare.

623

624 **References**

625 Aalto, E.A., Barry, J.P., Boch, C.A., Litvin, S.Y., Micheli, F., Woodson, C.B., De Leo, G.A.,

626 2020. Abalone populations are most sensitive to environmental stress effects on adult

627 individuals. *Marine Ecology Progress Series*, 643:75-85. <https://doi.org/10.3354/meps13320>

628 Aonuma, H., Mezheritskiy, M., Boldyshev, B., Totani, Y., Vorontsov, D., Zakharov, I., Etsuro,

629 I., Dyakonova, V., 2020. The Role of Serotonin in the Influence of Intense Locomotion on

630 the Behavior Under Uncertainty in the Mollusc *Lymnaea stagnalis*. *Frontiers in Physiology*,

631 11 : 221. doi:10.3389/fphys.2020.00221

632 Auzoux-Bordenave, S., Badou, A., Gaume, B., Berland, S., Helléouet, M.-N., Millet, C.,

633 Huchette, S., 2010. Ultrastructure, chemistry and mineralogy of the growing shell of the

- 634 European abalone *Haliotis tuberculata*. Journal of Structural Biology, 171 : 277-290.
635 <https://doi.org/10.1016/j.jsb.2010.05.012>
- 636 Auzoux-Bordenave, S., Wessel, N., Badou, A., Martin, S., M'Zoudi, S., Avignon, S., Roussel,
637 S., Huchette, S., Dubois, P., 2020. Ocean acidification impacts growth and shell
638 mineralization in juvenile abalone (*Haliotis tuberculata*). Marine Biology, 167:11.
639 <https://doi.org/10.1007/s00227-019-3623-0>
- 640 Avignon, S., Auzoux-Bordenave, S., Martin, S., Dubois, P., Badou, A., Coheleach, M., Richard,
641 N., Di Giglio, S., Malet, L., Servili, A., 2020. An integrated investigation of the effects of
642 ocean acidification on adult abalone (*Haliotis tuberculata*). ICES Journal of Marine Science,
643 77: 757-772. <https://doi.org/10.1093/icesjms/fsz257>
- 644 Beniash, E., Ivanina, A., Lieb, NS., Kurochkin, I., Sokolova, I.M., 2010. Elevated level of carbon
645 dioxide affects metabolism and shell formation in oysters *Crassostrea virginica*. Marine
646 Ecology Progress Series, 419: 95–108. doi: 10.3354/meps08841.
- 647 Bilbao, A., Tuset, V., Viera, M., Courtois de Viçose, G., Fernandez-Palacios, H., Haroun, R.,
648 Izquierdo, M., 2010. Reproduction, fecundity, and growth of abalone (*Haliotis tuberculata*
649 *coccinea*, Reeve 1846), in the Canary Islands. Journal of Shellfish Research, 29 : 959-967.
650 doi:10.2983/035.029.0430.
- 651 Bolton, J.J., Robertson-Andersson, D.V., Shuuluka, D., Kandjengo, L., 2009. Growing *Ulva*
652 (Chlorophyta) in integrated systems as a commercial crop for abalone feed in South Africa:
653 a SWOT analysis. Journal of Applied Phycology, 21: 575–583. doi:10.1007/s10811-008-
654 9385-6
- 655 Boulais, M., Soudant, P., Le Goïc, N., Quéré, C., Boudry, P., Suquet, M., 2015. Involvement of
656 mitochondrial activity and OXPHOS in ATP synthesis during the motility phase of
657 spermatozoa in the pacific oyster, *Crassostrea gigas*. Biology of Reproduction, 93: 1–7. doi:
658 10.1095/biolreprod.115.128538
- 659 Boulais, M., Suquet, M., Arsenault-Pernet, E. J., Malo, F., Queau, I., Pignet, P., Ratiskol, D., Le
660 Grand, J., Huber, M., Cosson, J., 2018. pH controls spermatozoa motility in the Pacific

- 661 oyster (*Crassostrea gigas*). *Biology Open*, 7: bio031427. Company of Biologists Ltd.
662 doi:10.1242/bio.031427
- 663 Byrne, M., Soars, N.A., Ho, M.A., Wong, E., McElroy, D., Selvakumaraswamy, P., Dworjanyn,
664 S. A., Davis, A.R., 2010. Fertilisation in a suite of coastal marine invertebrates from SE
665 Australia is robust to near-future ocean warming and acidification. *Marine Biology*, 157 :
666 2061–2069. <https://doi.org/10.1007/s00227-010-1474-9>.
- 667 Byrne, M., Ho, M., Wong, E., Soars, N.A., Selvakumaraswamy, P., Shepard-Brennand, H.,
668 Dworjanyn, S.A., Davis, A.R., 2011. Unshelled abalone and corrupted urchins: development
669 of marine calcifiers in a changing ocean. *Proceedings of the Royal Society B, Biological*
670 *Sciences*, 278, 2376–2383. doi: 10.1098/rspb.2010.2404.
- 671 Byrne, M., Fitzner, S., 2019. The impact of environmental acidification on
672 the microstructure and mechanical integrity of marine
673 invertebrate skeletons. *Conservation Physiology*. [https://doi.org/10.1093/](https://doi.org/10.1093/conphys/coz062)
674 [conphys/coz062](https://doi.org/10.1093/conphys/coz062)
- 675 Cook, P.A., 2016. Recent trends in worldwide abalone production. *Journal of Shellfish Research*,
676 35: 581–583. <https://doi.org/10.2983/035.035.0302>
- 677 Courtois de Viçose, G., Viera, M. P., Bilbao, A., Izquierdo, M. S., 2007. Embryonic and larval
678 development of *Haliotis tuberculata coccinea* Reeve: an indexed micro-photographic
679 sequence. *Journal of Shellfish Research*, 26: 847–854. [https://doi.org/10.2983/0730-](https://doi.org/10.2983/0730-8000(2007)26[847:EALDOH]2.0.CO;2)
680 [8000\(2007\)26\[847:EALDOH\]2.0.CO;2](https://doi.org/10.2983/0730-8000(2007)26[847:EALDOH]2.0.CO;2)
- 681 Courtois de Viçose G., Viera, M.P., Huchette, S., Izquierdo, M.S., 2012. Larval settlement, early
682 growth and survival of *Haliotis tuberculata coccinea* using several algal cues. *Journal of*
683 *Shellfish Research*, 31: 1189–1198. doi: 10.2983/035.031.0430.
- 684 Crim, R.N., Sunday, J.M., Harley, C.D.G., 2011. Elevated seawater CO₂ concentrations impair
685 larval development and reduce larval survival in endangered northern abalone (*Haliotis*
686 *kamtschatkana*). *Journal of Experimental Marine Biology and Ecology*, 400 :272–277. doi:
687 10.1016/j.jembe.2011.02.002.

- 688 Cunningham, S.C., Smith, A.M., Lamare, M.D., 2016. The effects of elevated pCO₂ on growth,
689 shell production and metabolism of cultured juvenile abalone, *Haliotis iris*. *Aquaculture*
690 *Research*, 47:2375–2392. doi: 10.1111/are.12684.
- 691 Curd, A., Pernet, F., Corporeau, C., Delisle L., Firth, L. B., Nunes, F.L.D., Dubois, S.F., 2019.
692 Connecting organic to mineral: How the physiological state of an ecosystem-engineer is
693 linked to its habitat structure, *Ecological Indicators*, 98: 49-60.
694 <https://doi.org/10.1016/j.ecolind.2018.10.044>.
- 695 Daume, S., Huchette, S., Ryan, S., Day, R.W., 2004. Nursery culture of *Haliotis rubra*: the effect
696 of cultured algae and larval density on settlement and juvenile production. *Aquaculture*, 236:
697 221-239. doi: 10.1016/j.aquaculture.2003.09.035.
- 698 Dickson, A.G., Millero, F.J., 1987. A comparison of the equilibrium constants for the
699 dissociation of carbonic acid in seawater media. *Deep Sea Research Part A. Oceanographic*
700 *Research Papers* 34, 1733-1743. doi: 10.1016/0198-0149(87)90021-5.
- 701 Dickson, A.G., Sabine, C.L., Christian, J.R. (Eds), 2007. Guide to Best Practices for Ocean CO₂
702 measurements. PICES Special Publication 3. 191pp. doi: 10.25607/OBP-1342
- 703 Doney, S.C., Fabry, V.J., Feely, R.A., Kleypas, J.A., 2009. Ocean acidification: The other CO₂
704 problem. *Annual Review of Marine Science* 1, 169-192.
705 doi:10.1146/annurev.marine.010908.163834.
- 706 Duquette, A., McClintock, J.B., Amsler, C.D., Pérez-Huerta, A., Milazzo, M., Hall-Spencer,
707 J.M., 2017. Effects of ocean acidification on the shells of four Mediterranean gastropod
708 species near a CO₂ seep. *Marine Pollution Bulletin*, 124 : 917-928.
709 <https://doi.org/10.1016/j.marpolbul.2017.08.007>.
- 710 Ekstrom, J.A., Suatoni, L., Cooley, S.R., Pendleton, L.H., Waldbusser, G.G., Cinner, J.E., Ritter,
711 J. Langdon, C., van Hooidek, R., Gledhill, D., Wellman, K., Beck, M., Brander, L., Rittschof,
712 D., Doherty, C., Edwards, P., Portela, R., 2015. Vulnerability and adaptation of US
713 shellfisheries to ocean acidification. *Nature Climate Change*, 5:207–214. doi:
714 10.1038/nclimate2508.

- 715 Ellis, R.P., Bersey, J., Rundle, S.D., Hall-Spencer, J.M., Spicer, J.I., 2009. Subtle but significant
716 effects of CO₂ acidified seawater on embryos of the intertidal snail, *Littorina obtusata*.
717 *Aquatic Biology*, 5:41–48. doi: 10.3354/ab00118.
- 718 Espinel-Velasco, N., Lamare, M., Kluibenschedl, A., Moss, G., Cummings, V., 2021. Ocean
719 acidification induces carry-over effects on the larval settlement of the New Zealand abalone,
720 *Haliotis iris*. *ICES Journal of Marine Science*, 78 (1), 340-348. doi:10.1093/icesjms/fsaa086.
- 721 Fitzer, S.C., Phoenix, V.R., Cusack, M., Kamenos, N.A., 2014. Ocean acidification impacts
722 mussel control on biomineralisation. *Science Report*, 4: 6218. doi: 10.1038/srep06218.
- 723 Gattuso, J.-P., Magnan, A., Billé, R., Cheung, W.W., Howes, E.L., Joos, F., Allemand, D., Bopp,
724 L., Cooley, S.R., Eakin, C.M., Hoegh-Guldberg, O., 2015. Contrasting futures for ocean and
725 society from different anthropogenic CO₂ emissions scenarios. *Science*, 349, aac4722. doi:
726 10.1126/science.aac4722.
- 727 Gaume, B., Denis, F., Van Wormhoudt, A., Huchette, S., Jackson, D. J., Avignon, S., Auzoux-
728 Bordenave, S., 2014. Characterisation and expression of the biomineralising gene *Lustrin A*
729 during shell formation of the European abalone *Haliotis tuberculata*. *Comparative*
730 *Biochemistry and Physiology Part B: Biochemistry and Molecular Biology*, 169: 1–8.
731 <http://dx.doi.org/10.1016/j.cbpb.2013.11.010>
- 732 Gazeau, F., Gattuso, J-P., Dawber, C., Pronker, A.E., Peene, F., Peene, J., Heip C.H.R.,
733 Middelburg, J.J., 2010. Effect of ocean acidification on the early life stages of the blue
734 mussel *Mytilus edulis*. *Biogeosciences*, 7: 2051–2060. doi: 10.5194/bg-7-2051-2010
- 735 Gazeau, F., Parker, L.M., Comeau, S., Gattuso, J-P., O'Connor, W.A., Martin, S., Pörtner, H-O.,
736 Ross, P.M., 2013. Impacts of ocean acidification on marine shelled molluscs. *Marine*
737 *Biology*, 160: 2207–2245. doi: 10.1007/s00227-013-2219-3.
- 738 Gran, G., 1952. Determination of the equivalence point in potentiometric titrations. Part II.
739 *Analyst*, 77: 661–671.

- 740 Grilo, T.F., Lopes, A.R., Sampaio, E., Rosa, R., Cardoso, P.G., 2018. Sex differences in oxidative
741 stress responses of tropical topshells (*Trochus histrio*) to increased temperature and high
742 pCO₂. *Marine Pollution Bulletin*, 131, A: 252-259, doi:10.1016/j.marpolbul.2018.04.031.
- 743 Guo, X., Huang, M., Pu, F., You, W., Ke, C., 2015. Effects of ocean acidification caused by
744 rising CO₂ on the early development of three molluscs. *Aquatic Biology*, 23: 147-157. doi:
745 10.3354/ab00615.
- 746 Gurr, S.J., Trigg, S.A., Vadopalas, B., Roberts, S.B., Putnam, H.M., 2021. Repeat exposure to
747 hypercapnic seawater modifies growth and oxidative status in a tolerant burrowing clam.
748 *Journal of Experimental Biology*, 224(13): jeb233932. doi: 10.1242/jeb.233932.
- 749 Hamdoun, A., Epel, D., 2007. Embryo stability and vulnerability in an always changing world.
750 *Proceedings of the National Academy of Sciences, USA*, 104: 1745-1750. doi:
751 10.1073/pnas.0610108104.
- 752 Haraldsson, C., Anderson, L. G., Hassellöv, M., Hulth, S., Olsson, K., 1997. Rapid, high-
753 precision potentiometric titration of alkalinity in ocean and sediment pore waters. *Deep Sea*
754 *Research, Part I, Oceanography Research Paper*, 44: 2031-2044. doi: 10.1016/S0967-
755 0637(97)00088-5.
- 756 Harney, E.D., Dubief, B., Boudry, P., Basuyaux, O., Schilhabel, M.B., Huchette, S.,
757 Paillard, C., Nunes, F.L.D., 2016. De novo assembly and annotation of the
758 European abalone *Haliotis tuberculata* transcriptome. *Marine Genomics*, 28: 11–16.
759 <https://doi.org/10.1016/j.margen.2016.03.002>.
- 760 Hatakeyama, D., Ito, E., 2000. Distribution and developmental changes in GABA-like
761 immunoreactive neurons in the central nervous system of pond snail, *Lymnaea stagnalis*.
762 *Journal of Comparative Neurology*, 418(3): 310-322. [https://doi.org/10.1002/\(SICI\)1096-
763 9861\(20000313\)418:3<310::AID-CNE6>3.0.CO;2-A](https://doi.org/10.1002/(SICI)1096-9861(20000313)418:3<310::AID-CNE6>3.0.CO;2-A)
- 764 Hendriks, I. E., Duarte, C. M., Álvarez, M., 2010. Vulnerability of marine biodiversity to ocean
765 acidification: A meta-analysis. *Estuarine, Coastal and Shelf Science*, 86: 157–164.
766 <https://doi.org/10.1016/j.ecss.2009.11.022>

- 767 Hernádi, L., 1994. Distribution and anatomy of GABA-like immunoreactive neurons in the
768 central and peripheral nervous system of the snail *Helix pomatia*. *Cell and Tissue Research*,
769 277(1): 189-198.
- 770 Hofmann, G. E., Barry, J. P., Edmunds, P. J., Gates, R. D., Hutchins, D. A., Klinger, T., Sewell,
771 M. A., 2010. The effect of ocean acidification on calcifying organisms in marine ecosystems:
772 An organism-to-ecosystem perspective. *Annual Review of Ecology, Evolution and*
773 *Systematics*, 41: 127–147. <https://doi.org/10.1146/annurev.ecolsys.110308.120227>
- 774 Huchette, S., Soulard, J.P., Koh, C.S., Day, R., 2004. Maternal variability in the blacklip abalone,
775 *Haliotis rubra* leach (Mollusca: Gastropoda): effect of egg size on fertilisation success.
776 *Aquaculture*, 231: 181-195. doi: 10.1016/j.aquaculture.2003.08.027.
- 777 Huchette, S., Clavier, J., 2004. Status of the ormer (*Haliotis tuberculata* L.) industry in Europe.
778 *Journal of Shellfish Research*, 23: 951-956.
- 779 IPCC, 2014. Summary for Policymakers. In: *Climate Change 2014: Impacts, Adaptation, and*
780 *Vulnerability. Part A: Global and Sectoral Aspects. Contribution of Working Group II to the*
781 *Fifth Assessment Report of the Intergovernmental Panel on Climate Change*. Cambridge
782 University Press, Cambridge, United Kingdom and New York, NY, USA, 1132 pp.
- 783 Jardillier, E., Rousseau, M., Gendron-Badou, A., Fröhlich, F., Smith, D.C., Martin, M.,
784 Helléouet, M.-N., Huchette, S., Doumenc, D., Auzoux-Bordenave, S., 2008. A
785 morphological and structural study of the larval shell from the abalone *Haliotis tuberculata*.
786 *Marine Biology*, 154 (4): 735-744. <https://doi.org/10.1007/s00227-008-0966-3>
- 787 Jing, J., Vilim, F. S., Wu, J. S., Park, J. H., Weiss, K. R., 2003. Concerted GABAergic actions
788 of *Aplysia* feeding interneurons in motor program specification. *Journal of Neuroscience*,
789 23(12): 5283-5294. doi: [10.1523/JNEUROSCI.23-12-05283.2003](https://doi.org/10.1523/JNEUROSCI.23-12-05283.2003)
- 790 Kavousi, J., Roussel, S., Martin, S., Gaillard, F., Badou, A., Di Poi, C., Huchette, S. Dubois P.,
791 Auzoux-Bordenave S., 2021. Combined effects of ocean warming and acidification on the
792 larval stages of the European abalone *Haliotis tuberculata*. *Marine Pollution Bulletin*, 175:
793 11313. <https://doi.org/10.1016/j.marpolbul.2021.113131>.

- 794 Kimura, R.Y.O., Takami, H., Ono, T., Onitsuka, T., Nojiri, Y., 2011. Effects of elevated pCO₂
795 on the early development of the commercially important gastropod, Ezo abalone *Haliotis*
796 *discus hannai*. Fisheries Oceanography, 20: 357-366. doi: 10.1111/j.1365-
797 2419.2011.00589.x.
- 798 Knudson, C., Benson, S., Geyer, C., Jones, G., 2021. Likelihood-based Inference for Generalized
799 Linear Mixed Models: Inference with the R Package glmm." Stat, 10 (1). [e339].
800 <https://doi.org/10.1002/sta4.339>.
- 801 Kroeker, K.J., Kordas, R.L., Crim, R., Hendriks, I.E., Ramajo, L., Singh, G.S., Duarte, C.M.,
802 Gattuso, J.-P., 2013. Impacts of ocean acidification on marine organisms: quantifying
803 sensitivities and interaction with warming. Global Change Biology, 19: 1884-1896. doi:
804 10.1111/gcb.12179.
- 805 Kurihara H., 2008. Effects of CO₂-driven ocean acidification on the early developmental stages
806 of invertebrates. Marine Ecology Progress Series, 373:275–284. doi: 10.3354/meps07802.
- 807 Kuznetsova, A., Brockhoff, P. B., Christensen, R. H. B., 2017. LmerTest Package: Tests in
808 Linear Mixed Effects Models. Journal of Statistical Software, 82(13): 1-26.
809 doi:10.18637/jss.v082.i13.
- 810 Le Roy, N., Marie, B., Gaume, B., Guichard, N., Delgado, S., Zanella-Cléon, I., Becchi, M.,
811 Auzoux-Bordenave S., Sire J.-Y., Marin F., 2012. Identification of two carbonic anhydrases
812 in the mantle of the European abalone *Haliotis tuberculata* (Gastropoda, Haliotidae):
813 Phylogenetic implications. Journal of Experimental Zoology, Part B: Molecular and
814 Developmental Evolution, 318: 353–367. doi: [10.1002/jez.b.22452](https://doi.org/10.1002/jez.b.22452).
- 815 Lerusalimsky, V. N., Balaban, P. M., 2001. Ontogenesis of the snail, *Helix aspersa*:
816 embryogenesis timetable and ontogenesis of GABA-like immunoreactive neurons in the
817 central nervous system. Journal of Neurocytology, 30(1):73-91. doi: [10.1023/a:1011921525359](https://doi.org/10.1023/a:1011921525359)
- 818 Li, J., Mao, Y., Jiang, Z., Zhang, J., Fang, J., Bian, D., 2018. The detrimental effects of CO₂-
819 driven chronic acidification on juvenile Pacific abalone (*Haliotis discus hannai*).
820 Hydrobiologia, 809: 297-308. <https://doi.org/10.1007/s10750-017-3481-z>.

- 821 Lowry, O. H., Rosebrough, N. J., Farr, A. L., Randall, R. J., 1951. Protein measurement with the
822 Folin phenol reagent. *Journal of Biological Chemistry*, 193(1):265-75.
- 823 Mazurais, D., Servili, A., Le Bayon, N., Gislard, S., Madec, L., Zambonino-Infante, J. L., 2020.
824 Long-term exposure to near-future ocean acidification does not affect the expression of
825 neurogenesis- and synaptic transmission-related genes in the olfactory bulb of European sea
826 bass (*Dicentrarchus labrax*). *Journal of Comparative Physiology, Part B*, 190(2): 161-167.
827 <https://doi.org/10.1007/s00360-019-01256-2>
- 828 Mehrbach, C., Culberson, C.H., Hawley, J.E., Pytkowicz, R.M., 1973. Measurement of the
829 apparent dissociation constants of carbonic acid in seawater at atmospheric pressure.
830 *Limnology and Oceanography*, 18:897–907. doi: 10.4319/lo.1973.18.6.0897.
- 831 Melzner, F., Gutowska, M.A., Langenbuch, M., Dupont, S., Lucassen, M., Thorndyke, M.C.,
832 Bleich M., Pörtner, H-O., 2009. Physiological basis for high CO₂ tolerance in marine
833 ectothermic animals: pre-adaptation through lifestyle and ontogeny? *Biogeosciences*
834 6:2313–2331. <https://doi.org/10.5194/bg-6-2313-2009>
- 835 Miller, M. W., 2019. GABA as a Neurotransmitter in Gastropod Molluscs. *Biological Bulletin*,
836 236(2): 144-156. doi:10.1086/701377.
- 837 Morash, A.J., Alter, K., 2015. Effects of environmental and farm stress on abalone physiology:
838 perspectives for abalone aquaculture in the face of global climate change. *Reviews in*
839 *Aquaculture* 7:1–27. <https://doi.org/10.1111/raq.12097>
- 840 Munari, M., Chemello, G., Finos, L., Ingrosso, G., Giani, M., Marin, M.G., 2016. Coping with
841 seawater acidification and the emerging contaminant diclofenac at the larval stage: A tale from
842 the clam *Ruditapes philippinarum*. *Chemosphere*, 160: 293-302,
843 doi:10.1016/j.chemosphere.2016.06.095.
- 844 Nicolas, J-L., Basuyaux, O., Mazurié, J., Thébault, A., 2002. *Vibrio carchariae*, a pathogen of
845 the abalone *Haliotis tuberculata*. *Diseases of Aquatic Organisms*, 50:35–43. doi:
846 10.3354/dao050035

- 847 Nilsson, G. E., Dixson, D. L., Domenici, P., McCormick, M. I., Sørensen, C., Watson, S-A.,
848 Munday, P. L., 2012. Near-future carbon dioxide levels alter fish behaviour by interfering
849 with neurotransmitter function. *Nature Climate Change*, 2(3): 201-204.
850 doi:10.1038/nclimate1352.
- 851 Noisette, F., Comtet, T., Legrand, E., Bordeyne, F., Davoult, D., Martin, S., 2014. Does
852 encapsulation protect embryos from the effects of ocean acidification? The example of
853 *Crepidula fornicata*. *PLoS ONE* 9(3): e9321. doi: 10.1371/journal.pone.0093021.
- 854 O'Leary, J.K., Barry, J.P., Gabrielson, P.W., Rogers-Bennett, L., Potts, D.C., Palumbi, S.R.,
855 Micheli, F., 2017. Calcifying algae maintain settlement cues to larval abalone following
856 algal exposure to extreme ocean acidification. *Science Report*, 7: 1-10.
857 <https://doi.org/10.1038/s41598-017-05502-x>
- 858 Onitsuka, T., Takami, H., Muraoka, D., Matsumoto, Y., Nakatsubo, A., Kimura, R., Ono, T.,
859 Nojiri, Y., 2018. Effects of ocean acidification with pCO₂ diurnal fluctuations on survival
860 and larval shell formation of Ezo abalone, *Haliotis discus hannai*. *Marine Environmental*
861 *Research*, 134: 28-36. doi: 10.1016/j.marenvres.2017.12.015.
- 862 Orr, J.C., Fabry, V.J., Aumont, O., Bopp, L., Doney, S.C., Feely, R.A., Gnanadesikan, A.,
863 Gruber, N., Ishida, A., Joos, F., Key, R.M, Lindsay, K., Maier-Reimer, E., Matear, R.,
864 Monfray, P., Mouchet, A., Najjar, R.G., Plattner, G.K, Rodgers, K.B., Sabine, C.L.,
865 Sarmiento, J.L., Schlitzer, R., Slater, R.D., Totterdell, I.J., Weirig, M.F., Yamanaka, Y.,
866 Yool, A., 2005. Anthropogenic ocean acidification over the twenty-first century and its
867 impact on calcifying organisms. *Nature*, 437:681–686. doi: 10.1038/nature04095
- 868 Parker, L.M., Ross, P.M., O'Connor, W.A., Borysko, L., Raftos, D.A., Pörtner, H-O., 2012. Adult
869 exposure influences offspring response to ocean acidification in oysters. *Global Change*
870 *Biology* 18: 82-92. <https://doi.org/10.1111/j.1365-2486.2011.02520.x>
- 871 Parker, LM., O'Connor, WA., Raftos, DA., Pörtner, H-O., Ross, P.M., 2015. Persistence of
872 Positive Carryover Effects in the Oyster, *Saccostrea glomerata*, following Transgenerational

- 873 Exposure to Ocean Acidification. PLoS ONE, 10 (7): e0132276.
874 doi:10.1371/journal.pone.0132276
- 875 Pereira, L., Lagos, J., Araya, F., 2007. Evaluation of three methods for transporting larvae of the
876 red abalone *Haliotis rufescens* Swainson for use in remote settlement. Journal of Shellfish
877 Research, 26(3): 777-781. doi:10.2983/0730-8000(2007)26[777:eotmft]2.0.co;2.
- 878 Pierrot, D.E., Lewis, E., Wallace, D. W. R., 2006. MS Excel program developed for CO₂ system
879 calculations. ORNL/CDIAC-105a. Carbon Dioxide Information Analysis Center. Oak Ridge
880 National Laboratory, US Department of Energy, Oak Ridge, Tennessee. doi:
881 [10.3334/CDIAC/otg.CO2SYS_XLS_CDIAC105a](https://doi.org/10.3334/CDIAC/otg.CO2SYS_XLS_CDIAC105a)
- 882 Przeslawski, R., Byrne, M., Mellin, C., 2015. A review and meta-analysis of the effects of
883 multiple abiotic stressors on marine embryos and larvae. Global Change Biology, 21: 2122-
884 2140. <https://doi.org/10.1111/gcb.12833>
- 885 Qui-Minet, Z.N., Delaunay, C., Grall, J., Six, C., Cariou, T., Bohner, O., Legrand, E., Davoult,
886 D., Martin, S., 2018. The role of local environmental changes on maerl and its associated
887 non-calcareous epiphytic flora in the Bay of Brest. Estuarine, Coastal and Shelf Science,
888 208: 140-152. <https://doi.org/10.1016/j.ecss.2018.04.032>
- 889 R Core Team, 2015. R Core Team: A language and environment for statistical computing.
890 Vienna, Austria, version 3.6.2. <https://www.R-project.org>.
- 891 Ross, P.M., Parker, L.M., O'Connor, W.A., Bailey, EA., 2011. The impact of ocean acidification
892 on reproduction, early development and settlement of marine organisms. Water 3: 1005–
893 1030. doi: 10.3390/w3041005.
- 894 Ross, P. M., Parker, L.M., Byrne, M., 2016. Transgenerational responses of molluscs and
895 echinoderms to changing ocean conditions. ICES Journal of Marine Science, 73: 537–549.
896 <https://doi.org/10.1093/icesjms/fsv254>
- 897 Strader, M.E., Wong, J.M., Hofmann, G.E., 2020. OA promotes broad transcriptomic responses
898 in marine metazoans: a literature survey. Frontiers in Zoology, 17: 7. doi:10.1186/s12983-
899 020-0350-9.

- 900 Swezey, D.S., Boles, S.E., Aquilino, K.M., Stott, H.K., Bush, D., Whitehead, A., Rogers-
901 Bennett, L., Hill, T.M., Sanford, E., 2020. Evolved differences in energy metabolism and
902 growth dictate the impacts of ocean acidification on abalone aquaculture. Proceedings of the
903 National Academy of Sciences, USA, 117: 26513-26519. doi: [10.1073/pnas.2006910117](https://doi.org/10.1073/pnas.2006910117)
- 904 Tahil, A.S., Dy, D.T., 2016. Effects of reduced pH on the early larval development of hatchery-
905 reared Donkey's ear abalone, *Haliotis asinina* (Linnaeus 1758). Aquaculture, 459: 137-142.
906 doi: [10.1016/j.aquaculture.2016.03.027](https://doi.org/10.1016/j.aquaculture.2016.03.027).
- 907 Thomas, J. T., Munday, P. L., Watson, S.-A., 2020. Toward a Mechanistic Understanding of
908 Marine Invertebrate Behavior at Elevated CO₂. Frontiers in Marine Science 7: 345. doi:
909 [10.3389/fmars.2020.00345](https://doi.org/10.3389/fmars.2020.00345).
- 910 Travers, M.-A., Basuyaux, O., Le Goïc, N., Huchette, S., Nicolas, J.-L., Koken, M., Paillard, C.,
911 2009. Influence of temperature and spawning effort on *Haliotis tuberculata* mortalities
912 caused by *Vibrio harveyi*: an example of emerging vibriosis linked to global warming.
913 Global Change Biology, 15: 1365-1376. doi: [10.1111/j.1365-2486.2008.01764.x](https://doi.org/10.1111/j.1365-2486.2008.01764.x).
- 914 Wessel, N., Martin, S., Badou, A., Dubois, P., Huchette, S., Julia, V., Nunes, F., Harney E.,
915 Paillard C., Auzoux-Bordenave S., 2018. Effect of CO₂-induced ocean acidification on the
916 early development and shell mineralization of the European abalone (*Haliotis tuberculata*).
917 Journal of Experimental Marine Biology and Ecology, 508: 52-63. doi:
918 [10.1016/j.jembe.2018.08.005](https://doi.org/10.1016/j.jembe.2018.08.005).
- 919 Widdicombe, S., Spicer, J.I., 2008. Predicting the impact of ocean acidification on benthic
920 biodiversity: What can animal physiology tell us? Journal of Experimental Marine Biology
921 and Ecology, 366:187–197. doi: [10.1016/j.jembe.2008.07.024](https://doi.org/10.1016/j.jembe.2008.07.024).
- 922 Wittmann, A.C., Pörtner, H.-O., 2013. Sensitivities of extant animal taxa to ocean acidification.
923 Nature Climate Change 3: 995-1001. doi: [10.1038/NCLIMATE1982](https://doi.org/10.1038/NCLIMATE1982).
- 924 Winter, B., 2013. Linear models and linear mixed effects models in R with linguistic applications.
925 arXiv:1308.5499.

- 926 Zhang, T., Qu, Y., Zhang, Q., Tang, J., Cao, R., Dong, Z., Wang, Q., Zhao, J., 2021. Risks to the
927 stability of coral reefs in the South China Sea: An integrated biomarker approach to assess
928 the physiological responses of *Trochus niloticus* to ocean acidification and warming. *Science*
929 of The Total Environment, 782: 146876. doi: [10.1016/J.SCITOTENV.2021.146876](https://doi.org/10.1016/J.SCITOTENV.2021.146876)
- 930 Zippay, M.L., Hofmann, G.E., 2010. Effect of pH on gene expression and thermal tolerance of
931 early life history stages of red abalone (*Haliotis rufescens*). *Journal of Shellfish Research*,
932 29: 429-439. doi: [10.2983/035.029.0220](https://doi.org/10.2983/035.029.0220).

Journal Pre-proof

- Abalone has experienced severe population decline worldwide due to overfishing, disease and climate change
- The effects of simulated OA were evaluated on reproduction and early life stages of European abalone (*Haliotis tuberculata*) through a transgenerational experiment.
- No carry-over effects were observed on abalone offspring following parental exposure to OA
- Larval and juvenile fitness were affected by low pH
- Species dispersion and survival may be compromised under future conditions, with potential negative consequences for European abalone populations.

Journal Pre-proof

Declaration of interests

The authors declare that they have no known competing financial interests or personal relationships that could have appeared to influence the work reported in this paper.

The authors declare the following financial interests/personal relationships which may be considered as potential competing interests:

Journal Pre-proof